COMBURA

NVV 2015

Book of Abstracts

NVV

KIVI NIRIA

PROGRAMME

- Keynote lecture: Fuel design for low emission engine combustion Stefan Pisching **READ**

PARALLEL SESSION 1 — New combustion systems / MILD combustion

- LES and DNS of autoignition in the Delft Jet-in-Hot Coflow burner with CH4/H2 **READ**
  Ebrahim Abtahizadeh, Jeroen van Oijen, Rob Bastiaans, Philip de Goey *(TU Eindhoven)*

- Numerical study of MILD spray combustion using OpenFOAM **READ**
  Likun Ma, Dirk Roekaerts *(TU Delft)*

- Development of Multi-Stage FGM Approach **READ**
  Ugur Göktolga, Jeroen van Oijen *(TU Eindhoven)*

- A preliminary simulation of flameless combustion in a single-burner furnace **READ**
  Xu Huang, Dirk Roekaerts *(TU Delft)*

- Hybrid Combustion System for Future Aero Engines **READ**
  Arvind Gangoli Rao *(TU Delft)*

PARALLEL SESSION 2 — Industrial and experimental combustion

- Research activities on pulverised coal injection into the Blast Furnace **READ**
  Stefan Born *(Tata Steel)*

- Investigating the Effects of Heat Exchanger Tubes on Flame Transfer Function in a Simplified Boiler **READ**
  Naseh Hosseini *(TU Eindhoven/Bekaert)*

- Thermo-acoustic modelling in a boiler using FEM **READ**
  Harshit Gupta, Joan Teerling *(Bekaert Combustion Technology)*

- Lowering the emissions of a waste incinerating boiler using the Stork AFA system **READ**
  Bart Venneker *(Stork Thermeq)*

- *Fate of Forgotten Fuel: High-Speed Laser-Induced Incandescence* **READ**
  Robbert Willems, Peter-Christian Bakker, Nico Dam *(TU Eindhoven)*

COMBURA NVV 2015

PARALLEL SESSION 3 — Laminar flames

Two-dimensional electric fields in methane-air flames on the heat flux burner
READ

Nico Speelman, Jeroen van Oijen *(TU Eindhoven),* **Nijso Beishuizen** *(Bosch)*

Effects of the mixture Lewis number on laminar flame stabilization and blow-off behavior
READ

Yuriy Shoshin, Rob Bastiaans, Philip de Goey *(TU Eindhoven)*

Detailed simulation and flamelet modeling of laminar premixed flames interacting with cold walls
READ

Daniel Mayer *(RWTH-Aachen),* **Nijso Beishuizen** *(Bosch Thermotechniek),*
Heinz Pitsch *(RWTH Aachen)*

PARALLEL SESSION 4 — Turbulence-chemistry-interaction modeling

Comparison of chemical mechanism, model flame and turbulence-chemistry interaction sub-models in FGM for Diesel combustion
READ

Casper Meijer, Ferry Tap *(Dacolt)*

Turbulent combustion modeling of a confined premixed methane/air jet flame using tabulated chemistry, RaNS and LES, including heat loss.
READ

Simon Gövert, Jim Kok *(U Twente)*

On the effect of LES sub-grid models for the opening angle of a swirling jet flow in a model gas-turbine combustor
READ

Giel Ramaekers, Ferry Tap *(Dacolt),* **Bendiks Jan Boersma** *(TU Delft)*

Keynote lecture: Still burning after all these years: better, cleaner, and less
READ

Simone Hochgreb *(University of Cambridge)*

COMBURA
NVV 2015

POSTER PRESENTATIONS

○ Experimental database on turbulent spray flames in hot-diluted coflow
   H. Correia Rodrigues, M.J. Tummers, E.H. van Veen, D.J.E.M.Roekaerts

READ

○ Response of premixed counterflow flame to a heaviside strain rate
   A.G. Iyer, J.A. van Oijen, J.H.M. ten Thije Boonkkamp

READ

○ The effect of the perforation geometry of plate burners on flame stability - Experimental and numerical approach
   S. Kruse, D. Mayer, P. Milz, N. Beishuizen, H. Pitsch

READ

○ Determination of the fractal dimension of silica aggregates in 1-D methane/hexamethyldisiloxane/air flames by light scattering measurements
   P.N. Langenkamp, H.B. Levinsky, A.V. Mokhov

READ

○ Large Eddy Simulation of MILD spray jet flames
   L. Ma, D.J.E.M. Roekaerts

READ

○ Heavy-Duty Diesel Spray in a High-Pressure, High-Temperature Vessel: Towards Spray-Wall Interaction
   N.C.J. Maes, N.J. Dam, L.M.T. Somers, G. Hardy

READ

○ Modelling Tar Conversion in a Partial Oxidation Reactor Using Flamelet Generated Manifolds
   J.C.A.M. Pennings, J.A. van Oijen, T. Kuipers, F. Melkert

READ

○ Combustion in Swirling Flows, Modelling of Premixed Turbulent Combustion in Swirling Flows using Large Eddy Simulations and Tabulated Chemistry
   M. Reintjes, W.J.S. Ramaekers, J.A. van Oijen, F.A. Tap

READ

○ Fate of Forgotten Fuel: High-speed Laser-Induced Incandescence
   **R.C. Willems, P.C. Bakker, N.J. Dam**

READ

Fuel design for low emission engine combustion

Stefan Pischinger, Institute for Combustion Engines, RWTH Aachen University

In the cluster of excellence "Tailor-Made Fuels from Biomass" at RWTH Aachen University, novel production pathways towards novel bio-based fuel components are investigated. The aim of the program is to develop and establish an interdisciplinary method named "Fuel Design" in which optimal fuel components are identified: these optima are characterized by both, a sustainable and energy-efficient production of the fuels from lignocellulosic biomass as well as a clean combustion with the highest efficiency possible.

In this presentation, the vision and establishment of the "Fuel Design Process" will be presented, focusing on the positive effects on the combustion characteristics of tailor-made fuels. In order to characterize the combustion relevant properties of novel fuels, dedicated measuring technologies like glow-plug measurements to investigate pre-ignition behavior have been developed and applied to the fuel candidates.

In the work of TMFB it could be proven that – when the right properties are considered – novel fuels with superior properties can be identified. In the gasoline engine, 2-butanone was found to allow for an efficiency increase at full load condition by more than 15 %, see the graphic below. For the Diesel engine, 1-octanol was identified as promising candidate to allow soot-free and lowest-NOx combustion.
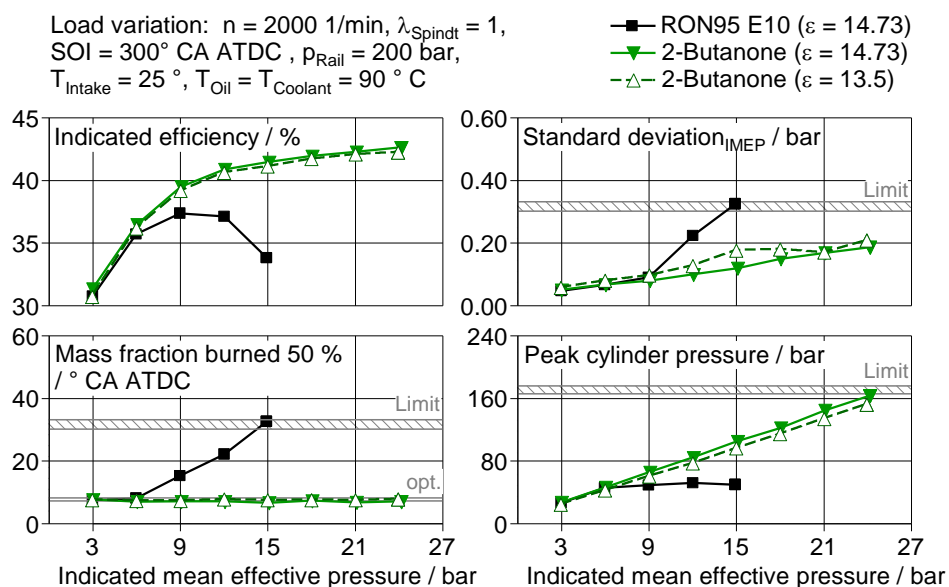
LES and DNS of autoignition in the Delft Jet-in-Hot Coflow burner with CH4/H2 fuels

S.E. Abtahizadeh, J.A. van Oijen, R.J.M. Bastiaans, L.P.H. de Goey
Eindhoven University of Technology
Combustion technology group, Mechanical engineering department
De Rondom 70, 5612 AP, Eindhoven, the Netherlands
E-mail: e.abtahizadeh@tue.nl

Key words: Turbulent combustion, DNS, LES, SGS modeling, Autoignition

ABSTRACT

Autoignition of a fuel mixture by a hot oxidizer plays an important role in Mild combustion; a clean combustion concept. Mild combustion has been introduced as a promising method to increase thermal efficiency and decrease NOx formation. In spite of the enormous potential of the Mild combustion regime, it has been mainly limited to lab-scale burners due to stabilization issues in practical burners. The stabilization mechanism of Mild combustion is often governed by autoignition of a fuel jet in a hot and diluted environment. This mechanism is highly sensitive to variations in the fuel and oxidizer composition and operating conditions. In the laboratory scale Mild burners (JHC burners), stabilization of reaction zone is very often occurred by autoignition. In some burners, methane-based fuel is enriched with H_2. Such conditions require sophisticated models which are able to predict complex autoignition events under significant preferential diffusion effects.

The Delft Jet-in-Hot Coflow (DJHC) burner is chosen as a test case in which methane base fuel has been enriched with 0%, 5%, 10% and 25% of H_2. Studied cases are summarized in Table 1. First, a novel numerical model is developed based on the FGM technique to account for preferential diffusion effects in autoignition. Such development is inevitable since investigations with detailed chemistry indicate that preferential diffusion affects strongly autoignition of the hydrogen enriched mixtures. Igniting Mixing Layer (IML) flamelets are introduced and analyzed to accommodate preferential diffusion effects in a flamelet database. The predictions of this model are then compared with results of the full chemistry mode by performing 3D DNS of igniting mixing layers. Figure 1 shows the comparison of predicted temperature rise ΔT for the Case D25H2 using detailed chemistry and various FGM models. Two FGM models are considered here which employ different types of manifolds: 1) A manifold based on igniting Counter-Flow flamelets (ICF-flamelets) 2) A manifold based on IML-flamelets. From Fig. 1, it is observed that computations based on IML Manifold provide more accurate results compared to those of ICF manifold against the solution of detailed chemistry.

Table 1. Temperature and molar composition of the fuel stream for the different cases. The oxidizer stream has the same composition for all cases: T = 1437 K, X_{O2} = 0.0485, X_{H2O} = 0.1452, X_{CO2} = 0.0727, X_{N2} = 0.7336.

Case	T(K)	X_{H_2}	X_{CH_4}	$X_{C_2H_6}$	X_{N_2}	ζ_{st}
D00H$_2$	448	0.00	0.813	0.037	0.15	0.0178
D05H$_2$	448	0.05	0.763	0.037	0.15	0.0179
D10H$_2$	448	0.10	0.713	0.037	0.15	0.0180
D25H$_2$	448	0.25	0.563	0.037	0.15	0.0183

In the next stage, the IML approach is implemented in LES of the H_2 enriched turbulent lifted jet flames of the DJHC experiments. A presumed β-PDF approximation together with a gradient based model has been used to account for turbulence-chemistry interaction. Figure 2 shows instantaneous Y_{OH} distributions. Predictions indicate formation, growth and convection of ignition kernels in perfect agreement with observations from measurements [1]. Observations from DNS and LES demonstrate that IML approach is a promising method to predict autoignition and preferential diffusion effects for Jet-in-Hot Coflow flames [2].
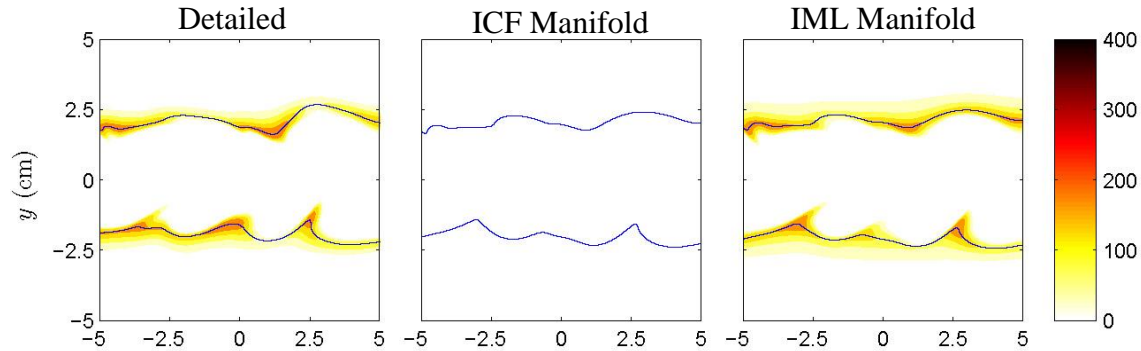
Figure 1 Comparison of the temperature rise ΔT obtained by 3D DNS of mixing layers using detailed chemistry, ICF and IML manifolds for the Case D25H2 at t=0.2 ms. Blue lines correspond to stoichiometric mixture fraction.
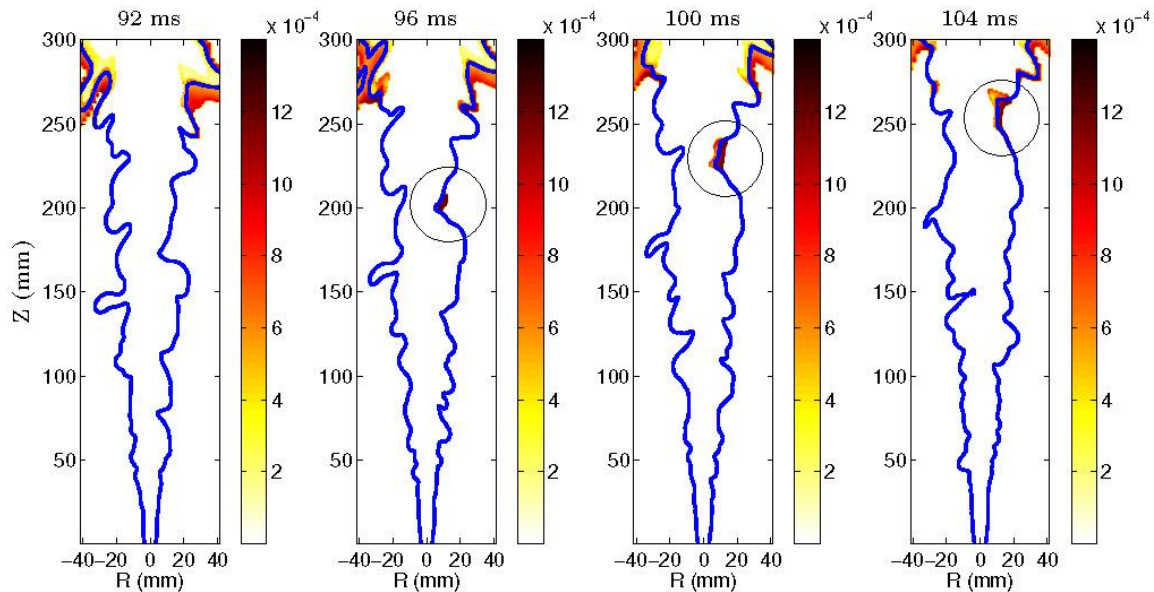

Figure 2 Computed instantaneous snapshots of Y_{OH} using the IML manifold for Case D00H2. Blue lines indicate stoichiometric mixture fraction.

Acknowledgments

References

[1] L.D.A. Arteaga, M.J. Tummers, E.H. van Veen, D.J.E.M. Roekaerts, *Effect of hydrogen addition on the structure of natural-gas jet-in-hot-coflow flames*, Proc. Combust. Inst. 35, (2014), pp. 3557-356.
[2] S.E. Abtahizadeh, *Numerical study of Mild combustion from laminar flames to Large Eddy Simulation of turbulent flames with Flamelet Generated Manifolds*, PhD Thesis, Eindhoven University of Technology (2014).

Numerical study of MILD spray combustion using OpenFOAM

L. Ma, D.J.E.M. Roekaerts

l.ma@tudelft.nl

Department of Process and Energy, Delft University of Technology, the Netherlands

Abstract

The Delft Spray-in-Hot-Coflow (DSHC) flame has been numerically studied with a new OpenFOAM solver developed by the authors, in which the Flamelet Generated Manifolds (FGM) model has been implemented, and used to account for the Turbulence-Chemistry Interaction (TCI). The enthalpy loss effect due to droplet vaporization is considered by employing an additional controlling parameter in the FGM library. This is realized by first constructing 2D FGM tables using counter-flow diffusion flame with reducing temperature at the oxidizer side. And then combining these 2D FGM tables to form the final 3D, (Z, C, η_h), FGM library, see Fig. (1). Different configurations for generating three dimensional non-adiabatic FGM library are tested.

Analysis of the DSHC experimental data suggested that flash boiling influences the atomization of liquid fuel in the DSHC burner. This introduces new challenges for specifying precise spray boundary conditions. A conditional injection model is proposed to provide precise spray information at the injector exit plane (Z=0 mm). In this conditional injection model, the droplets have an asymmetric distribution around the spray half angle, in agreement with experimental observations. Also, the possible range of droplet injection angle is conditioned upon the droplet size (mass). Droplet initial velocity magnitude is scaled such that it peaks at the spray half angle direction and reaches a minimum at the edge of the spray cloud. A schematic of this conditional droplet injection approach is given in Fig. (2).

The results obtained showed that the conditional droplet injection model significantly improves the prediction of all the properties examined compared to standard injection model. Comparison between Unsteady Reynolds Averaged Navier Stokes (URANS) and Large Eddy Simulation (LES) is made, and it is found that the LES predicted similar gas phase velocity and better temperature profiles compared to experimental data than URANS, due to better resolved turbulence field and mixture fraction variance. Strong droplet-flame interaction was shown to exist in the DSHC flame. Large droplets have ballistic trajectories at the early stage of their lifetime, and can penetrate the flame and survive until far downstream outside the main reaction region. Movement of these large droplets strongly deform the shape of the flame. A 3D instantaneous flame structure and spray cloud is given in Fig. (3). Rapid evaporation of droplets in the reaction region may also cause local quenching. Small droplets are quickly convected towards the central region and vanish soon, forming a fuel rich and high temperature condition in the center. These phenomena have been captured with the LES/non-adiabatic FGM modeling approach developed by the authors.
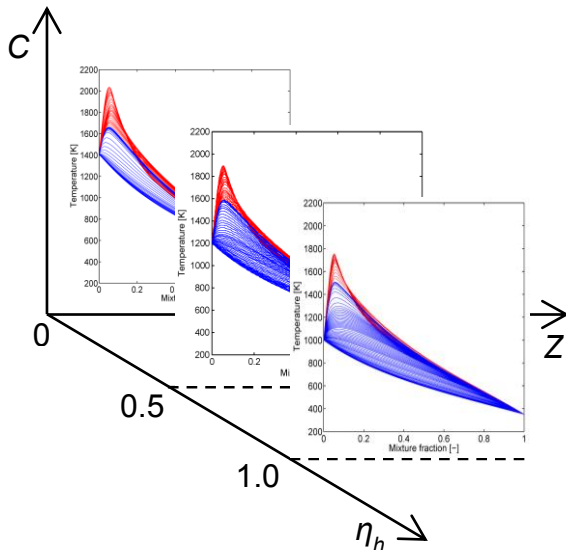
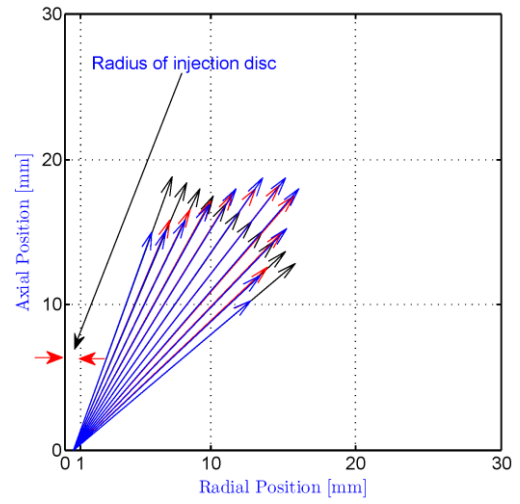Figure 1. Three dimensional (Z,C,η_h) non-adiabatic FGM library
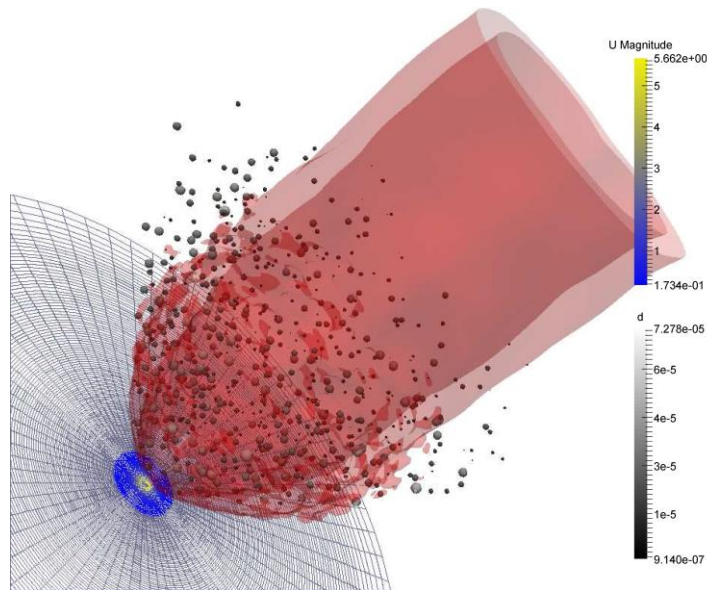

Figure 2. Schematic of conditional droplet injection

Figure 3. Instantaneous 3D spray flame structure and isosurface of $Y_{OH} = 0.001$. Droplets are scaled and colored with their diameter, bottom plate is colored with the gas phase velocity

Development of Multi-Stage FGM Approach

M. Ugur Goktolga [†], Jeroen A. van Oijen [†]

[†] Mechanical Engineering Department, Eindhoven University of Technology

Contact: m.u.goktolga@tue.nl j.a.v.oijen@tue.nl

Moderate or intense low-oxygen dilution (MILD) combustion is a relatively new technology which provides both high fuel-efficiency and low emissions. In this concept, the products of combustion are recirculated and mixed with the reactants, resulting in a hot and diluted oxidizer and/or fuel. When the preheating is so high that the mixture auto-ignites and the dilution is so high that the temperature increase in the combustion chamber is lower than the auto-ignition temperature, the process is called MILD combustion [1]. The peak temperature occurring in MILD combustion is considerably lower than that of traditional combustion, which suppresses NO_x emissions greatly. In addition, the combustion takes place in a homogenous manner.

It is not clear if the flamelet assumption is valid or in particular if flamelet generated manifolds (FGM) is applicable to MILD combustion since its characteristics are quite different than conventional combustion systems. To assess this, an *a priori* FGM analysis of MILD combustion was conducted using 1D flames. Firstly, the HM1 case of the experiments of Dally et al. [2] was simulated using igniting mixing layers (IML) [3]. In the simulation, DRM19 reaction mechanism was used and constant Lewis numbers were employed. Later, using the results of the simulation, several FGM tables were created with different progress variable (PV) selections. To test the success of each table: PV and mixture fraction (Z) were calculated at every grid point and time step in the detailed simulation; parameters like species mass fractions, temperature and source term of PV were looked up from the corresponding table; these looked up parameters were compared to their calculated counterparts from the detailed simulation; an error term for each parameter, P_i, was calculated as:

$$\epsilon_i = \frac{\frac{1}{N}\sqrt{\sum_{k=1}^{N}(P_i^{Detailed} - P_i^{FGM})^2}}{\frac{1}{N}\sum_{k=1}^{N}|P_i^{Detailed}|}$$

where N is the number of grid points; and the error term is examined as a function of time. The emphasis was put on the prediction of source term of PV, since its miscalculation will lead to a wrong look-up and thus an inaccurate modeling. The error terms for various PV definitions are given in Figure 1.
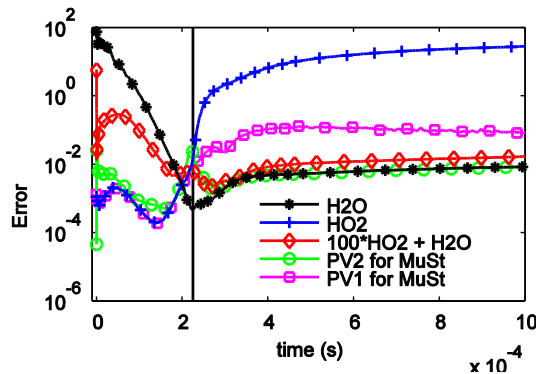

Figure 1. The error in predicting the source term of PV for various PV definitions. The vertical black line shows the start of the ignition

As seen in Figure 1, H_2O fails as PV in the pre-ignition region with the huge error terms at the beginning of the simulation. This is because while the precursors like HO_2 is formed in the pre-ignition period of MILD combustion, the product species like H_2O do not vary much and hence cannot represent this stage of combustion. On the other hand, HO_2 can represent the pre-ignition stage successfully, while it fails in the oxidation stage due to its consumption and resulting non-monotonicity. Following these findings, we have come up with the idea of using different PVs for different stages of combustion; multistage FGM (MuSt) method.

In MuSt approach, every stage of combustion (pre-ignition, oxidation, post-combustion) is represented using a different PV. An FGM table is generated for each stage using the corresponding PV, which stores the source terms of all the PVs. During the actual FGM simulation, transport equations for all the PVs are solved simultaneously. Depending on the values of PVs and the limits of the tables, the table to be looked up is determined.

For the current case, it was determined to use two PVs; one for the pre-ignition and another for the oxidation region. HO_2 was selected as PV_1 and H_2O as PV_2. The first table was generated until HO_2 fails to be monotonic, i.e., until its maximum value is reached in Z–space. The second table was generated using the flamelets from there on. The value of PV_2 is used to determine the switching between the tables: if PV_2 is smaller than its minimum value in the second table, look up from the first table; else, look up from the second table. The *a priori* analysis was repeated using this formulation and the results were promising, as seen in Figure 1. In addition, an actual simulation was performed and the main results are presented in Figure 2.
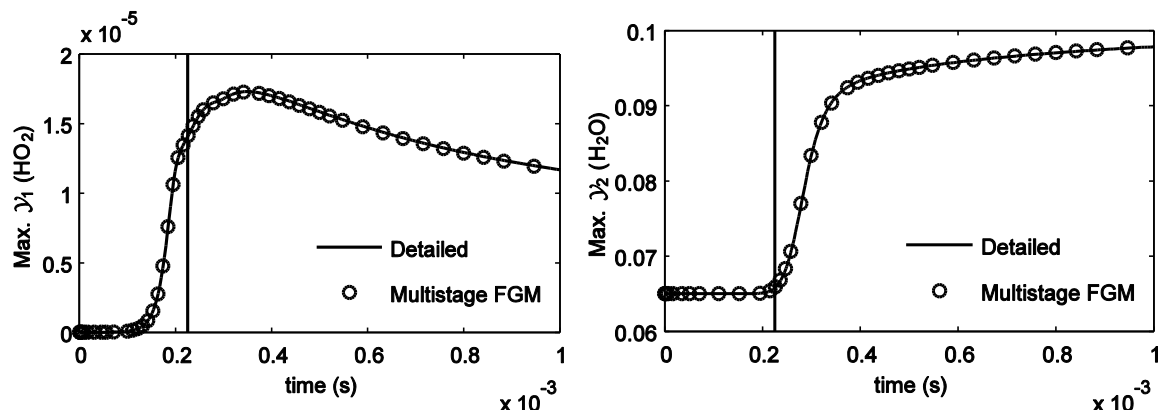

Figure 2. The evolution of the maximum values of PVs in the detailed and multistage FGM simulations. The vertical black line shows the start of the ignition.

Figure 2 demonstrates that MuSt approach is successful in modeling MILD combustion of non-premixed type in a 1D setting. It is worth noting that standard FGM calculations using a single PV have either numerically failed or have not resulted in any ignition for the current case.

We have shown here that MuSt method is a promising tool in modeling MILD combustion. It can also be used in other areas which include auto-ignition like diesel combustion, or which require emission prediction in the post-combustion zone.

References:

[1] A. Cavaliere, M. de Joannon, Prog. Energy and Combust. Sci. 30 (2004) 329–66.
[2] B. B. Dally, A. Karpetis, R. S. Barlow, Proc. Combust. Inst. 29 (2002) 1147–54.
[3] E. Abtahizadeh, Numerical study of Mild combustion, PhD thesis, Eindhoven University of Technology, Eindhoven, 2014.

A preliminary simulation of flameless combustion in a single-burner furnace

Xu Huang[*] and Dirk Roekaerts

Department of Process and Energy, Delft University of Technology

Introduction

Flameless combustion, also known as MILD combustion, was first developed to suppress thermal NOx formation in high temperature heating industrial furnaces using preheated combustion air. Flameless combustion will occur when fresh air (and/or fuel) streams are diluted with high temperature combustion products before reactions take place.

There is a large number of studies on flameless combustion and these studies can be classified into three categories based on the setups: jet in hot co-flow[1,2], single-burner furnace[3–5] and semi-industrial furnace[6]. Jet in hot co-flow mimics only certain conditions found in flameless combustion, and semi-industrial furnaces are very difficult for detailed measurements. A single burner furnace is most appropriate to experimentally and numerically study the principles of flameless combustion.

This study is a preliminary numerical investigation on flameless combustion in a single-burner furnace.

Setup description

Figure 1 shows the 3d geometry of the single-burner furnace being built in Delft University of Technology. The combustion chamber has a square cross section of 320×320 mm^2 and a height of 630 mm. A Rekumat recuperative Flame-Flox burner is placed at the bottom of the chamber. Fuel and air are injected through the central fuel tube (4.5 mm in diameter) and four air tubes. Flue gas goes out through the square ring exit and is then introduced into the recuperator. An air cooled plate is placed on the top of the chamber and acts as a heat sink. The furnace is designed with 3 quartz windows providing full optical access to the interior of the chamber. To avoid elaborate optical calibration, the burner is moved vertically inside the chamber, and optics, sensors and cameras for LDA, PIV, PLIF and CARS measurements are fixed.

---
[*]x.huang-2@tudelft.nl

① : REKUMAT M150 recuperative burner
② : burner nozzle
③ : fuel inlets
④ : air inlets
⑤ : recuperator outlet
⑥ : additional flue gas exits
⑦ : optical windows
⑧ : insulation walls
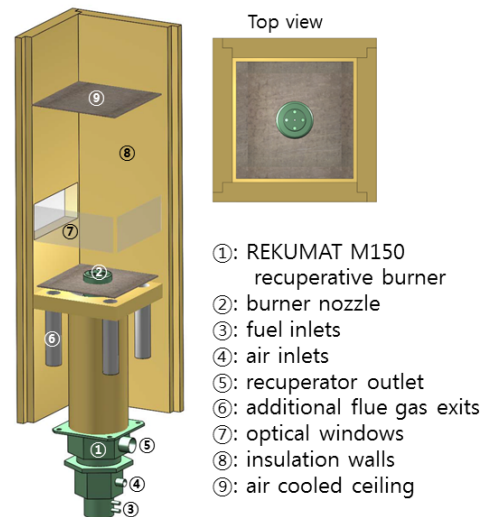⑨ : air cooled ceiling

Figure 1: 3d diagram of the furnace.

Numerical Methods

Numerical simulation was performed using the commercial package ANSYS Fluent 15. Nonadiabatic steady flamelet model, nonadiabatic flamelet generated manifold (FGM) model and eddy dissipation concept (EDC) model were employed. The detailed chemical kinetic mechanism (GRI-Mech 3.0) was employed with the first two models, and the Smooke skeleton mechanism for methane was used to reduce computational time in the EDC model. RNG $k-\epsilon$ and realizable $k-\epsilon$ model are used for turbulence closure. Radiation is modelled with discrete ordinate method with weighted-sum-of-gray-gases radiative properties.

Current results

Comparison of combustion models

Strong recirculation is present in the furnace. Flue gas is entrained into high-speed fuel and air jets. Both steady flamelet and FGM model predict an unrealistic OH in the region adjacent to air nozzle exits, and OH level is much stronger than that in EDC model, as
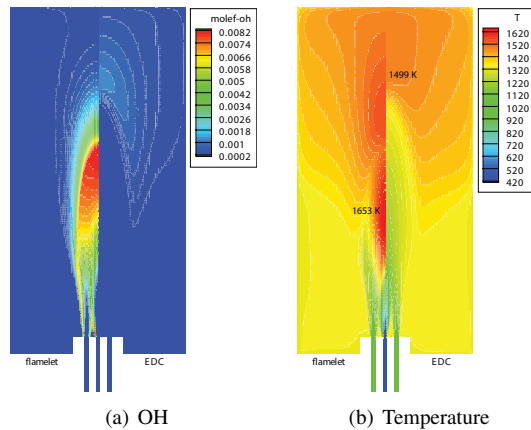
(a) OH (b) Temperature

Figure 2: Temperature and OH distribution: wall temperature is 1300 K

shown in figure 2(a). The peak temperature predicted in steady flamelet model is about 150 K higher than that in EDC model.

Comparison of turbulence models

Both the realizable and RNG $k - \epsilon$ models have substantial improvements over the standard $k - \epsilon$ model when the flow features include strong streamline curvature, vortices, and rotation[7]. In the comparison of the flow patterns predicted by RNG and realizable $k-\epsilon$ model, the latter one predicts less spreading rate and less decay of momentum, and this results in a stronger recirculation zone further downstream. In this case, heat is mainly released in the recirculation zone.

Effects of wall temperature

The wall boundaries in four cases were set as fixed temperature between 1200 K and 1500 K. Since high wall temperature leads to high temperature inside the furnace, fuel and air are preheated quicker and this results in reaction zone shifts from downstream to upstream. Combustion characteristics then are approaching conventional flame. This means that fuel does not have enough time to mix with flue gas before reactions are initiated.

Cooling in another two cases (wall temperature is 1300 K) is simulated by setting cooling ceiling at 1000 and 1100 K, respectively. The heat sinks are estimated as ∼7.2 kW and ∼5.7 kW in these two cases. Cooling does not have significant effects on combustion characteristics, but peak temperature decrease ∼50 K and ∼36 K, respectively.

The results at different wall temperatures show flame structure is sensitive to the temperature inside the furnace. Therefore, to be more realistic, convection and radiation were considered at wall outer surface rather than fixed wall temperature.

Summary

- Combustion characteristics are sensitive to the temperature inside the furnace, and this is associated with heat transfer at the walls.

- Flamelet based models need to be reformulated for combustion with strong recirculation in furnace, e.g. by considering the flue gas as the third stream.

- Flame structure is significantly affected by flow patterns, a proper turbulence model should be chosen.

References

[1] Ashoke De, Ernst Oldenhof, Pratap Sathiah, and Dirk Roekaerts. Numerical simulation of Delft-Jet-in-Hot-Coflow (DJHC) flames using the eddy dissipation concept model for turbulence-chemistry interaction. *Flow, Turbulence and Combustion*, 87(4):537–567, 2011.

[2] Paul R. Medwell, Peter A. M. Kalt, and Bassam B. Dally. Simultaneous imaging of OH, formaldehyde, and temperature of turbulent nonpremixed jet flames in a heated and diluted coflow. *Combustion and Flame*, 148(1-2):48–61, 2007.

[3] P. J. Coelho and N. Peters. Numerical simulation of a MILD combustion burner. *Combustion and Flame*, 124:503518, 2001.

[4] Szegö G.G., B.B. Dally, and G.J. Nathan. Scaling of NOx emissions from a laboratory-scale MILD combustion furnace. *Combustion and Flame*, 154:281–295, 2008.

[5] A. S. Verssimo, A. M. A. Rocha, and M. Costa. Operational, combustion, and emission characteristics of a small-scale combustor. *Energy and Fuels*, 25:2469–2480, 2011.

[6] E. S. Cho, D. Shin, J. Lu, W. de Jong, and D. J. E. M. Roekaerts. Configuration effects of natural gas fired multi-pair regenerative burners in a flameless oxidation furnace on efficiency and emissions. *Applied Energy*, 107:25–32, 2013.

[7] Ansys fluent 15.0 theory guide.

Hybrid Combustion System for Future Aero Engines

Arvind G. Rao
Associate Professor, Faculty of Aerospace Engineering, TU Delft

THE MULTI FUEL BLENDED WING BODY

The ACARE vision for European aviation in the year 2050 is to reduce CO_2 emission by 75%, NO_x emission by 90%, and noise emission by 65% [1]. This objective can only be achieved by dramatic improvement of both aero engine and aircraft. The Multi Fuel Blended Wing Body (MF-BWB) aircraft investigated in the EU sponsored AHEAD project (http://www.ahead-euproject.eu/) has the potential to meet the ambitious ACARE goals. The proposed MF-BWB configuration can be seen in Fig. 1. The main features of the aircraft are

- Carrying around 300 passengers for 14,000 km
- Ability to carry multiple-fuel, such as LNG/LH2 and Kerosene
- Utilizing Boundary Layer Ingestion (BLI) technology
- Ability to reduce CO_2, NO_x and noise emissions according to the ACARE requirements
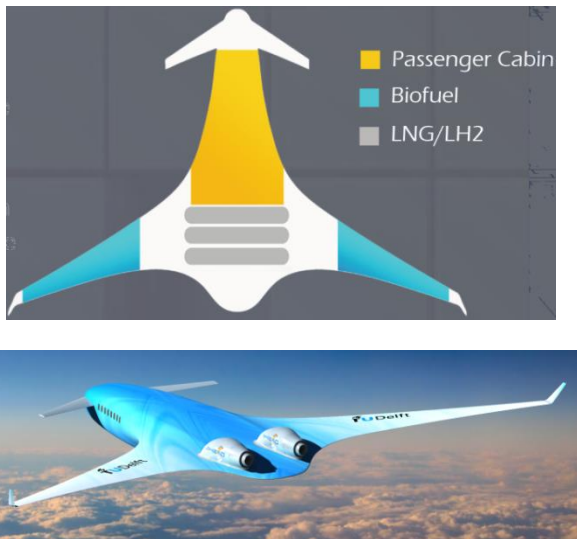

Figure 1: The AHEAD MF-BWB Aircraft

THE HYBRID ENGINE CONCEPT

In order to exploit this unique opportunity provided by the above mentioned MF-BWB aircraft, a novel engine concept, called as Hybrid Engine has been conceived. The schematic of the engine is presented in Fig. 2. The proposed hybrid engine is a combination of several technologies. The main features of this aircraft engine are as follows:
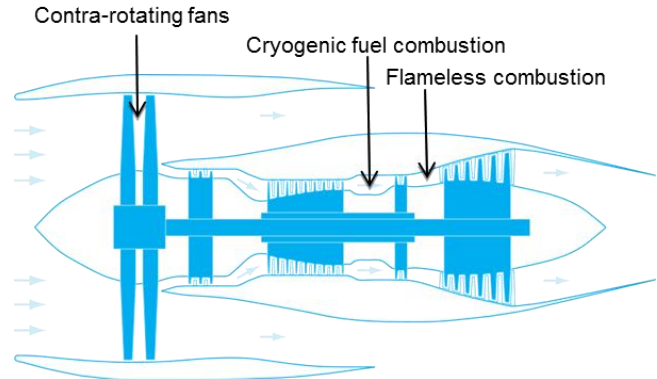

Figure 2: Schematic of Hybrid Engine [2]

- **Counter rotating fans:** to better sustain the non-uniform inflow caused by Boundary Layer Ingestion (BLI) techniques [3].
- **Dual Combustion Chamber**: The first combustion chamber (located between the HPC and HPT) burns cryogenic fuel (such as LH2/LNG) in a vaporized state, whereas, the second combustor is an Inter-stage Turbine Burner (ITB) and uses kerosene/biofuels in the flameless combustion mode. Since the flammability limit for Hydrogen / Methane is wider than for kerosene, the combustion in the first combustion chamber can take place at very lean conditions, and is beneficial from NOx emission perspective.
- **Flameless Combustion**: Using H2/CH4 in the first combustion chamber increases the concentration of H2O and reduces O2 concentration within the gases, thereby creating a high temperature vitiated environment at the inlet of ITB. This is beneficial to obtain Flameless Combustion (FC) regime as shown in Fig. 3. This helps to minimize emissions of CO, NOx, UHC, and soot [4].
- **Bleed Air Cooling System**: This system allows exploiting the cooling capacity provided by the cryogenic fuel to enhance the thermodynamic efficiency of the cycle by reducing the amount of compressor bleed air required for turbine cooling [5].
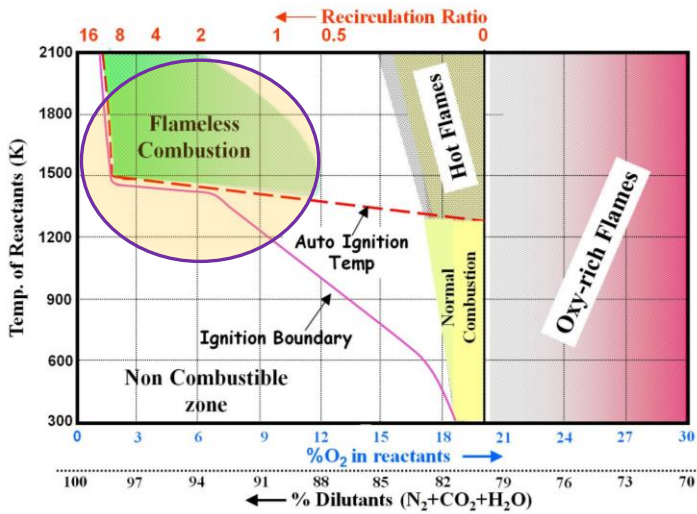
Figure 3: Schematic of different combustion regimes including flameless combustion [4]

THE HYBRID COMBUSTION SYSTEM

Of the various types of technologies associated with hybrid engine, the design and development of combustion system is of critical importance. For the AHEAD project this development was carried out for the LH2 combustor at TU Berlin and flameless combustor at Technion, Israel. Figure 4 shows the general flow field prevalent inside the swirl stabilized combustor. The combustor is connected to swirl generator (mixing tube) where the fuel is premixed with the air and is split into swirled component and axial air injection. The premixed flame gets stabilized at the exit of the mixing tube.
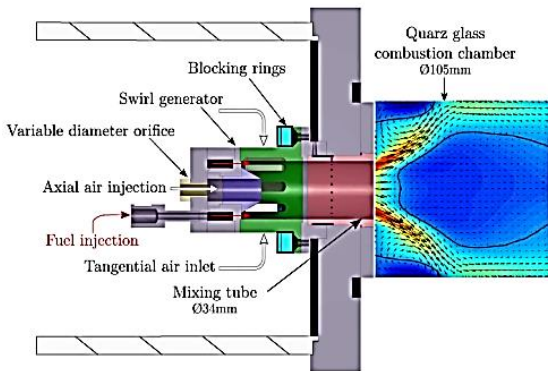

Figure 4: Schematic diagram of flow field inside the hydrogen combustor [6].

Figure 5 shows the flow field characteristics of second combustion chamber. The flow coming from HPT is split into two streams one used for combustion of fuel and other acts as a dilution air at the exit. The uniform temperature distribution inside the combustion chamber shows combustion taking place in a distributed regime which is the feature of the flameless combustion.
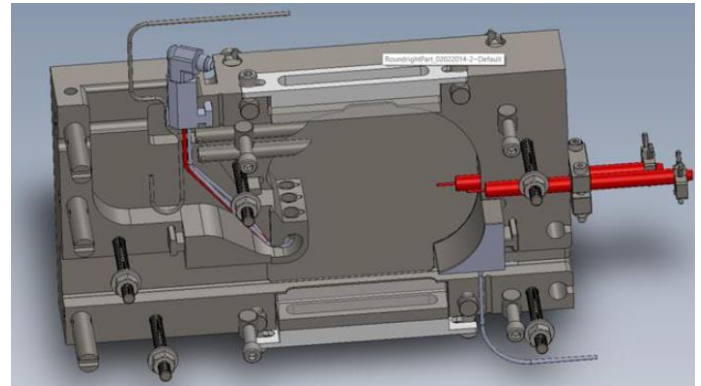

Figure 5: Schematic of flow path in the inter-turbine flameless combustor.

REFERENCES

[1]. ACARE, 2010, "Flightpath 2050 Europe's Vision for Aviation", Report of the High Level Group on Aviation Research.

[2]. A. Gangoli Rao, F. Yin and J.P. van Buijtenen, "A Hybrid Engine Concept for Multi-fuel Blended Wing Body", *Aircraft Engineering and Aerospace Technology*, Vol. 86 (6), Sept 2014.

[3]. C. Huo, N. Gonzalez Diez and A. Gangoli Rao "Numerical Investigations on the Conceptual Design of a Ducted Contra Rotating Fan", *Proceedings of ASME Turbo Expo 2014*. Düsseldorf, GT2014-26292.

[4]. Rao, G. A. and Levy, Y., 2010, "A New Combustion Methodology for Low Emission Gas Turbine Engines", *proceedings of the 8th HiTACG conference*, July 5-8, Poznan.

[5]. van Dijk, I.P., Rao, A.G., and van Buijtenen, J.P., 2009, Stator cooling & hydrogen based cycle improvements. *Proceedings of ISABE 2009*. Montreal.

[6]. Reichel, T. G., Terhaar, S., Paschereit, O. C., 2015, "Increasing Flashback Resistance in Lean Premixed Swirl-Stabilized Hydrogen Combustion by Axial Air Injection", *J. Eng. Gas Turbines Power* 137(7), 071503 (2015) (9 pages); Paper No: GTP-14-1522; doi:10.1115/1.4029119.

Research activities on pulverised coal injection into the Blast Furnace

S. Born*, J. van der Stel, T. Peeters

*Stefan.Born@tatasteel.com
Tata Steel, Research and Development, P.O. Box 10.000, 1970 CA IJmuiden, The Netherlands

Key words: blast furnace, coal injection, combustion, gasification, coal conversion

Tata Steel is a top ten global steel producer with one of their steel plants in IJmuiden, the Netherlands. Our integrated steel plants process iron ore (iron oxides) to liquid iron in blast furnaces.

As counter-current reactors, blast furnaces (**figure 1**) depend on lumpy materials, such as agglomerated iron ores (sinter/pellets) and coke. Coke, made from coking coals, is a carbonaceous material which supplies carbon to produce heat for the endothermic reduction reactions and acts as reaction partner for oxygen, bound in the iron oxides.

A major goal of the process optimisation is the decrease of the coke rate, e.g. by replacing it with fine coal, which is injected into the bottom of the blast furnace through lances.
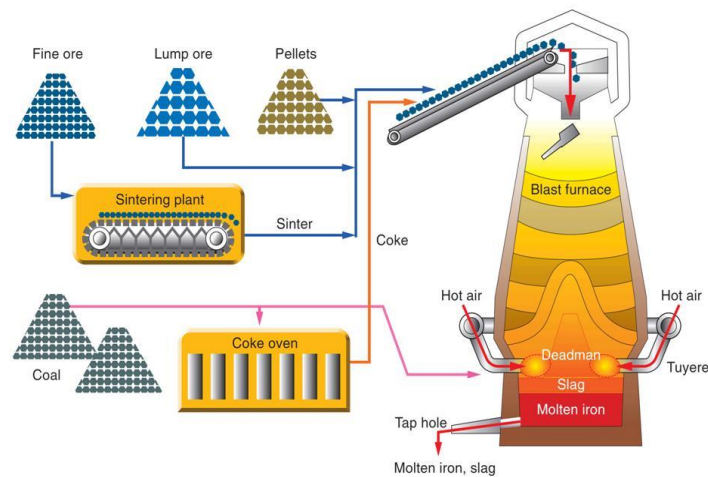

Figure 1: Blast furnace and supplemental plants [1]

The coal dust is being injected into the pre-heated hot blast and converts into CO_2 and finally CO, **figure 2**.

For an efficient usage of the injected coal, a proper consumption by flash-pyrolysis, combustion and gasification is essential. Otherwise, an accumulation of the un-burnt carbon in the furnace can lead to negative side effects on process performance and stability.

Therefore, the reactivity of coal as well as char needs to be considered.

$$C_{(s)} + \tfrac{1}{2} O_{2(g)} = CO_{(g)}$$
$$H_2O + C = H_2 + CO$$
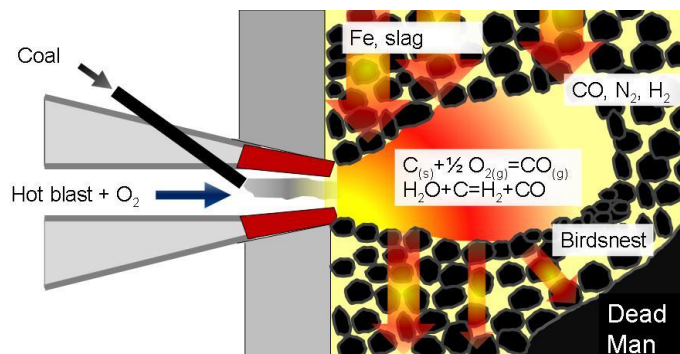
Figure 2: Combustion/gasification zone (Raceway)

Tata Steel has a long experience in expanding the limits of coal injection rate to far above 200 kg/t$_{HM}$ [2], **figure 3**.

The first experiments investigating coal combustion behaviour of different coals under conditions simulating injection into a blast furnace were conducted in the early eighties in a combustion test rig [3]. They revealed that a full combustion of coals is not possible, which is however desirable to avoid problems caused by combustion residue inside the blast furnace.
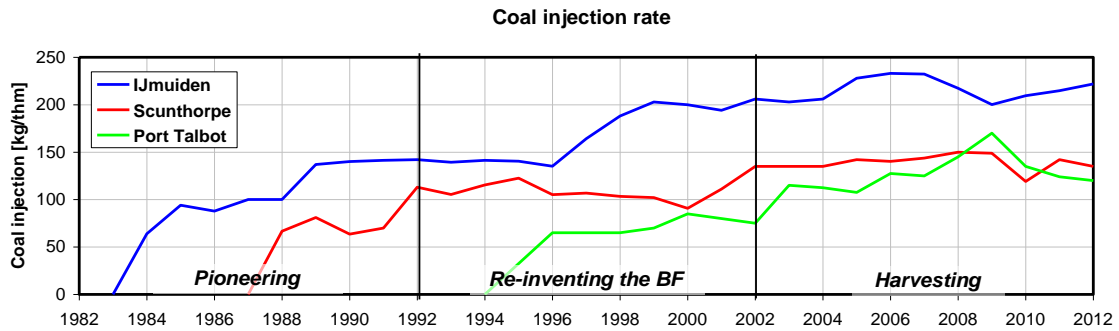
Figure 3: History of coal injection ramp-up at Tata Steel Europe [2]

To investigate conversion of coal in raceway and shaft, the coal char gasification was included in the current research program, making use of various laboratory investigations and research facilities.

With an increase of injection rates to above 200 kg/t_{hm}, process problems can occur [4, 5], such as an increasing pressure drop in the furnace, high carbon carry-over into the off-gas and increased hearth temperatures.

To rank coals and to try predicting their behaviour in the blast furnace, different methods have been used in the past: Usually the combustion/conversion degree is regarded as an important parameter, along with a minimal amount of un-burnt carbon and optimised characteristics.

An overview of the Tata Steels coal injection research is shown in **figure 4**.
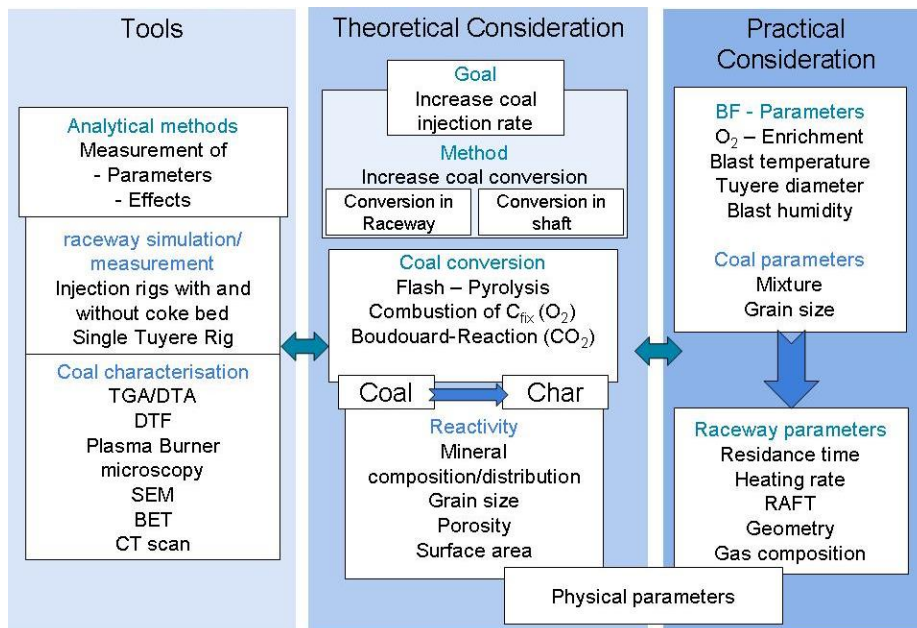
Figure 4: Overview scheme of application of coal injection research

The presentation will point out Tata Steels approach about combining different research facilities to support its knowledge on injection coals and effects on blast furnace performace.

Literature

[1] Y. Okuno: "Nippon Steel News, No. 316 May 2004", http://www.nsc.co.jp

[2] J. van der Stel, K. Meijer, T. Peeters, L. Bol, G. Tijhuis, D. Collins, I. Vaughan: "Three decades of coal injection at Tata Steel Europe"; 4th International Conference on Process Development in Iron and Steelmaking; 10-13 June 2012, Lulea, Sweden

[3] S. Bortz: "Coal injection into the Blast Furnace"; EUR 8544, Luxembourg; Office for Official Publications of the European Communities, 1982

[4] H. L. Toxopeus, A.G. S. Steeghs, J. F. C. van den Boer: "PCI at the Start of the 21st Century". ISS 60th Ironmaking Conference Proceedings; Baltimore, 2001

[5] H. L. Toxopeus, G. Danloy, R. Franssen, O. Havelange, C. Franssen, "Massive Injection of Coal and Super oxygenated Blast into the Blast Furnace"; EUR 20298, Luxembourg, Office for Official Publications of the European Communities, 2002

Investigating the Effects of Heat Exchanger on Flame Transfer Function in a Simplified Boiler

Naseh Hosseini[1,2,*], Viktor Kornilov[1], O.J. Teerling[2], Ines Lopez Arteaga[1,3] and L. P. H. de Goey[1]

[1] Eindhoven University of Technology, Mechanical Engineering Department, Eindhoven, the Netherlands.
[2] Bekaert Combustion Technology BV, Assen, the Netherlands.
[3] KTH Royal Institute of Technology, Department of Aeronautical and Vehicle Engineering, Stockholm, Sweden
[*] E-mail: n.hosseini@tue.nl

Abstract

The goal of the present work is to investigate the effects the heat exchanger can have on the acoustic response of the flames (flame transfer function) in a boiler. In compact condensing boilers the distance between the burner and heat exchanger is small enough to cause intense interactions. That is why we constructed a simplified CFD model of a boiler to study various cases with different distances between the burner and heat exchanger. Results show that the flame transfer function changes considerably when the flame impinges on the heat exchanger tube. The gain can acquire values above one for low frequencies due to incomplete combustion and the phase can be increased because of flame deformation and stretch. These results help analyze the acoustic behavior of the flames in such situations with more detail.

Introduction

Lean premixed combustion is widely used in industry mainly for the purpose of lowering emissions. It is well known that such systems are prone to thermoacoustic instabilities [1,2]. In thermoacoustic analysis of such systems the Flame Transfer Function (FTF) approach has gained extra attention due to its simplicity and good agreement with experimental data [3,4]. Most of the studies on flame transfer functions treat the flames as a separate acoustic element in the chain of other elements such as ducts, area changes, cavities and boundaries, leading to a so-called Network Model for modelling the acoustic response of the whole system. However, in situations such as compact condensing boilers intense hydrodynamic and thermal interactions take place between the burner and the heat exchanger and they cannot be treated separately.

The goal of the present work is to investigate how the presence of the heat exchanger in the vicinity of the flames can affect the flame transfer function. A simplified CFD model is created to simulate boiler conditions with a perforated plate burner and a tube heat exchanger. The dimensions and boundary conditions of the model are shown in Figure 1.
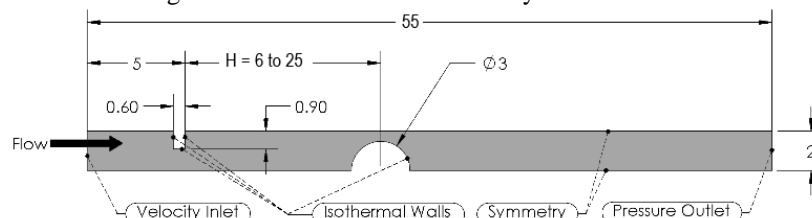

Figure 1. Numerical domain dimensions and boundary conditions.

We calculate the flame transfer function using velocity perturbations at the inlet in the form of a step profile with 5% increase (from 0.8 to 0.84m/s) as input, and heat release rate of the flames as output. We perform simulations for different distances (H = 6, 7, 8, 10 and 25mm) between the top surface of the burner deck and the center of the heat exchanger tube. All the walls of the burner deck are considered isothermal at 520°C, which is obtained from experiments, and the heat exchanger surface temperature is 70°C to prevent condensation and boiling. The details of the meshing and numerical scheme can be found in [5].

Results and Discussion

The contours of reaction rate (kmol/m^{3}s) and temperature (°C) for different distances between the burner and heat exchanger are shown in Figures 2(a) and (b), respectively. For 25mm distance the flow and temperature around the flame are unaffected by the presence of the tube and this case would be the same as when there is no heat exchanger. This behavior continues until 10mm and based on the classification introduced by Zhang et al. [6] these two cases exhibit a conical mode. However, for 8mm the flame shape starts deforming due to flow distortions and merging of flame temperature jump and heat exchanger thermal boundary layer, showing the envelope mode. Moving the heat exchanger 1mm closer will split the flame front and create cool central core mode. Further decrease of the distance will not exhibit other modes introduced by Zhang et al. since the classification has been performed for flames

impinging on flat plates. However, too close distances can cause intense flame quenching or stabilizing downstream of the tube, but these cases are not of practical importance and thus not studied here.
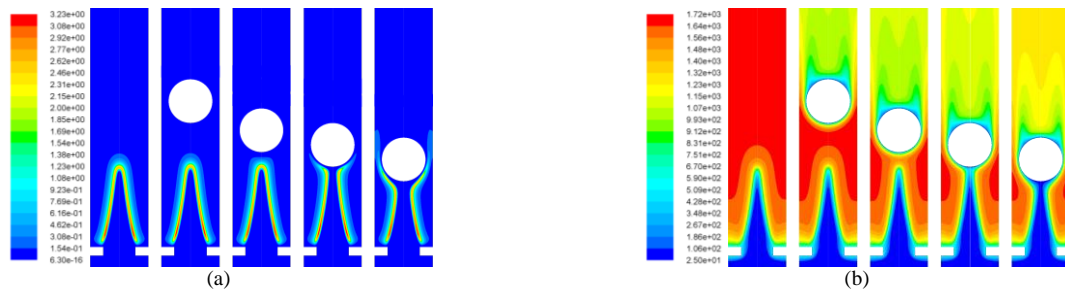

Figure 2. Contours of (a) reaction rate [kmol/m3s] and (b) temperature [°C] for H = 25mm, 10mm, 8mm, 7mm and 6mm, from left to right.

Figure 3 shows the gain and phase of flame transfer function for all cases. We can see that in the 25 and 10mm cases the flame responses are almost identical to the case without any heat exchanger. The gain for the 8mm case has a decrease, but follows a similar behavior between 100 and 700Hz. The phase and therefore time delay for all these three cases is almost the same, except above 700Hz for which the 8mm case has a slightly larger phase. This can be attributed to the flow distortions upstream of the tube and the fact that in this case it can take longer for fluctuations to convect through the flame. The same explanation describes the overall larger phase for the 7mm case.
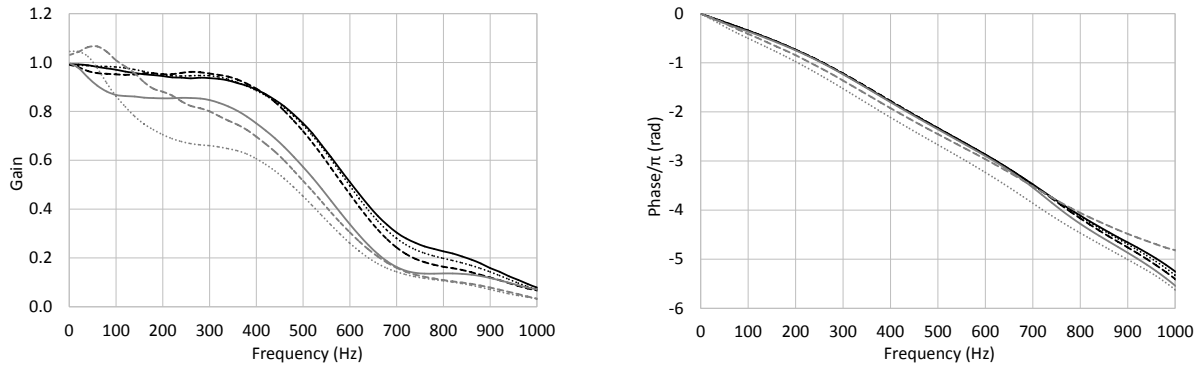

Figure 3. The gain and phase of the flame transfer function for the NoHex case (▬▬) and the cases with H = 25mm (•••••), 10mm (▬ ▬),
8mm (▬▬), 7mm (•••••) and 6mm (▬ ▬).

For the 6mm case a part of the flame is deformed towards the high velocity region between the tubes and therefore this part of the flame has a shorter convective time. This is why the phase for this case is not as large as the 7mm case. The gain for the 6 and 7mm cases exhibits a different behavior. It starts from a value larger than one, which is not normal for flame transfer function. We need to keep in mind that unity gain at 0Hz only occurs when complete combustion happens, i.e. 5% increase in inlet velocity leads to 5% increase in heat release of the flame. However, when the tube penetrates the flame some amount of unburnt CH_4 leaves the flame through the thermal boundary layer around the tube. This amount decreases by increasing velocity due to shrinkage of the boundary layer. This causes more than 5% increase in the heat release of the flame and thus a gain of more than one at 0Hz. These conditions that exist for low frequencies can enhance the thermoacoustic instabilities.

This paper is a short communication of an ongoing study and more detailed results will be orally presented.

Acknowledgement

References

[1]   Noble, A. C., King, G. B., Laurendeau, N. M., Gord, J. R., Roy, S., *Combustion Science and Technology*, **184** (3), 293-322, 2012.
[2]   Maria Luiza Bondar, *Acoustically Perturbed Bunsen Flames*, Doctor of Philosophy Thesis, Eindhoven University of Technology, 2007.
[3]   Kornilov, V., Rook, R., ten Thije Boonkkamp, J. H. M., de Goey, L. P. H., *Combustion and Flame*, **156** (10), 1957-1970, 2009.
[4]   Duchaine, F., Boudy, F., Durox, Daniel, Poinsot, Thierry, *Combustion and Flame*, **158** (12), 2384-2394, 2011.
[5]   Hosseini, N., Kornilov, V., Teerling, O. J., Lopez Arteaga, I., de Goey, L. P. H., *ICSV21*, Beijing, China,13-17 July, 2014.
[6]   Y. Zhang, K.N.C. Bray, Combustion and Flame, **116**, 671-674, 1999.

Thermo-acoustic modelling in a boiler using FEM

O.J. Teerling[1] and P.G.M. Hoeijmakers[,2]

[1] Bekaert Combustion Technology BV, Assen, The Netherlands.
[2] Mechanical Engineering Department, Eindhoven University of Technology, Eindhoven, The Netherlands
[*] E-mail: joan.teerling@bekaert.com

Abstract

The aim of the current work is to present a model and an approach that can be used in predicting thermo-acoustic instabilities in a realistic boiler geometry. Thermo-acoustic instabilities in boiler development are often one of the last problems that are resolved since they depend on many components in the flue gas way of a boiler system.

In the current work commercial FEM software COMSOL was used to calculate a thermo-acoustic stability map. A realistic boiler geometry comprising a heat exchanger with parallel flue gas channels and cylindrical burner is presented. The results of the numerical calculations were compared against thermo-acoustic observations on the real boiler. Besides the stability map, the locations where the acoustic pressure reaches maximum values were used to validate the model. Both the stability map and the acoustic pressure peaks show good agreement with observations on the real boiler .

Introduction

Lean premixed combustion is widely driven by the trend of lowering NOx emissions. It is well known that such systems are prone to thermo-acoustic instabilities (TAI) [1,2]. Prediction of thermo-acoustic behavior in boilers is generally performed by using a network approach. In such approach, individual simplifications of the several components are defined based on the geometry and are modelled as building blocks. These are then mathematically connected by e.g. multiplying the individual transfer matrix of each component. In the end a stability map of the complete system is generated. Although even detailed information about the flame (the Flame Transfer Function (FTF)) can be incorporated, the network approach is fast in calculating the stable and unstable eigenfrequencies. However this method is usually quite laborious. Moreover, a skilled person is required to set up a case and interpret the generated data. Let alone defining measures (such as geometrical changes or include resonators) reduce or loose the thermo-acoustic instabilities from this data is even more difficult. The approach presented here is more user-friendly in terms of case setup and the results can more easily be read and interpreted.

The current work was initiated by the cowork of Bekaert with the TU Eindhoven in the STW project 10430. In this project a start was made to study the accuracy of the current methods in predicting TAI in an realistic boiler geometry. The geometry studied was of a residential boiler with a flat burner and a single flue gas channel in the heat exchanger. Using a network model approach it was found that the majority of the predictions was correct even without any information on the FTF.
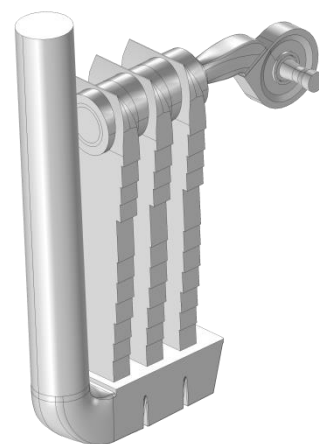

Figure 1. Geometry setup

Setup and modelling

The geometry case studied in this work is depicted in Figure 1. The first main difference from the residential boiler case is that the current geometry consists of a heat exchanger with a cylindrical burner rather than a flat burner . The second difference is that is the flue gases flow in parallel channels rather than in just one flue gas way.

The other components modelled are regular boiler components such as fan, gas valve, burner hood, sump and chimney. The gas volumes of each component are simplified and then connected in 3DCAD. For the heat exchanger a one-dimensional temperature profile over the height is imposed. For every other component an estimated uniform temperature is assumed, which corresponds to normal operating conditions. The open ends (inlet and outlet) are simply modelled using an end reflection coefficient R = -1. All the other boundaries are modelled as a hard wall.

The time delay in the burner is modelled by an acoustic velocity dependent monopole (source) using the N-τ approach [3] in an annulus-shaped volume around the burner tube. In the current study no detailed information on the FTF is used . The time delay τ is assumed to be constant for all frequencies and is used as a variable input parameter. In this way it is possible to get an good impression of the instabilities and the sensitivity of the

instabilities to the time delay which is related to the equivalence ratio of the gas-air mixture. The eigenmodes related to a given frequency are visualized by plotting the absolute value of the acoustic pressure on the domain walls.

The geometry used in this study is depicted in Figure 1. Starting from the left one can see the venturi, fan, burner hood, burner volume, heat exchanger, sump and exhaust. This corresponds to the way they are usually assembled in a boiler geometry.

Results

In the finite-element analysis, the eigenfrequencies in the 3D-geometry are calculated using an eigenvalue solver by the commercial software Comsol [4,5]. From a product development point of view it is mainly of interest what resonance frequencies can occur are and how unstable these are. The real part of this calculated eigenfrequency indicates the resonance frequency whereas the imaginary part indicate the growth rate. The resonance frequencies are non-dimensionalized by dividing them by the first resonance frequency of the system with no time delay. For the current case the non-dimensional eigenfrequencies are plotted in Figure 2. The unstable modes are plotted as circles, where size of the circle indicates the size of the growth rate. It can be seen that the most unstable eigenfrequencies are present for several time delays, indicating they are expected to be observed in operating the boiler, independent of the equivalence ratio. When looking at
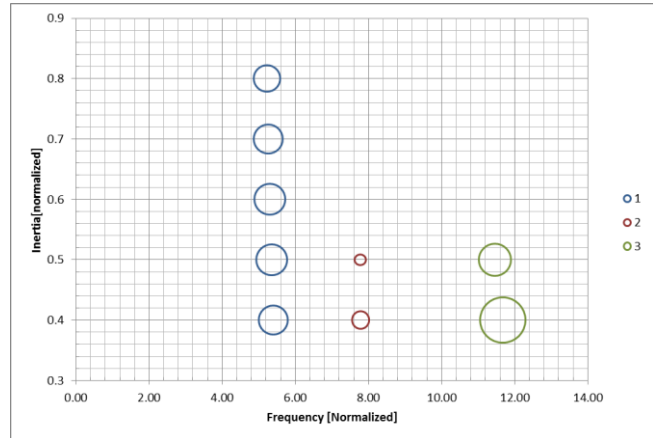

Figure 2. Ball plot of stable and unstable eigenfrequencies

the eigenmodes around a certain unstable frequency it can be observed that the qualitative impression of the pressure field is very much alike. An example of one eigenmode for different time delays is given in Figure 3.

The results of the eigenfrequencies were compared against the frequencies observed in the lab. It was found that the predicted unstable frequencies f > 1 were very much in line with the experimental observations. Also, when trying to reduce the instability by taking measures in the vicinity of a pressure peak location, it appeared to be most effective.
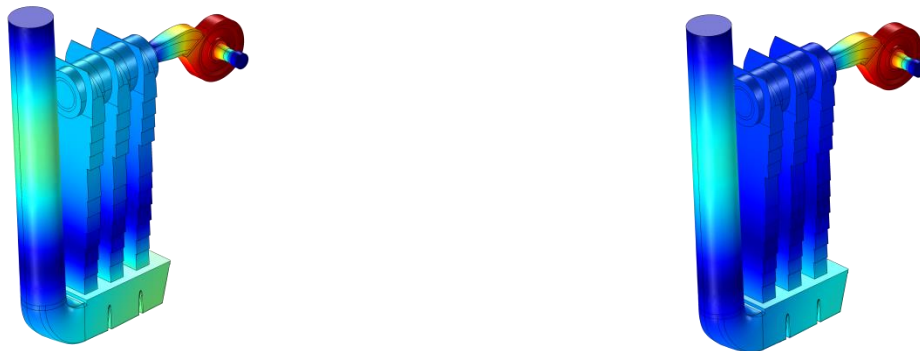
Figure 3. Contour plots of | p'| (local scale) on the geometry walls for τ = 0.4 and 0.8 for f = 4.5

References

[1] Noble, A. C., King, G. B., Laurendeau , N. M., Gord, J. R., Roy, S., *Combustion Science and Technology*, **184** (3), 293-322, 2012.
[2] Maria Luiza Bondar, *Acoustically Perturbed Bunsen Flames*, Doctor of Philosophy Thesis, Eindhoven University of Technology, 2007.
[3] Crocco, L. *12th Symp. (Int.) on Combustion* 85-99, 1969.
[4] Nicoud, F. Benoit, L., Sensiau, C., Poinsot, T. *AIAA Journal* **45** (2), 426-441,2007.
[5] Camporeale SM, Fortunato B, Campa G. *J of Eng. for Gas Turbines and Power*, **133**, 1-32, 2011.

Lowering the emissions of a waste incinerating boiler using the STORK AFA system
B.C.H. Venneker, J.N.A. Koomen
Stork Thermeq, P.O.Box 33, 7550 AA Hengelo, the Netherlands

Different techniques for lowering the emissions of NOx are available for combustion engineers, like burner modification, natural gas reburning, flue gas recirculation, selective (non)-catalytic reduction, fuel-staging and air-staging. When boilers or furnaces are to be retrofitted, not every technique is cost-effective or possible. Furthermore, for applicable techniques the combustion engineer has to deal with the limits of the particular site, e.g. size of the boiler, availability of auxiliaries.

In this presentation it is shown how Computational Fluid Dynamics is used to optimize a chosen NOX-reduction technique, after fire air(AFA) injection. With this technique, burners are operated generally under substochiometric conditions. The additional air that is needed for complete burn-out is then fed into the boiler a few meters downstream of the burner. Optimization of the exact way of injecting the after fire air is necessary as insufficient mixing will cause large emissions of CO and unburned hydrocarbons.

In this particular project the AFA-system consist of an air channel, protected by concrete, which is lead through the windbox and burner front wall into the furnace. In the furnace the air flow is splitted to the furnace left side and furnace right side. Next over the height of the furnace, the AFA is injected through different ports. The boiler is a waste incinerator with as feedstock a variety of liquid and gaseous wastes, next to natural gas, hydrogen, diesel and heavy fuel oil. In the simulations only combustion of natural gas was treated in order to reduce the complexity of the simulation. In the optimization study the number of ports and particularly the angle of injection is varied to find the optimal solution. Best results were obtained by varying the injection angle of the different ports in such a way that the rotation of the burner-air is followed.

During commissioning it was found that the AFA-system performed even better than expected: steam-injection into the flame to cool the flame temperature which was thought to be necessary at high loads, was not needed at all. After commissioning of the unit an independent company proved that the emissions of NOx, CO, SO2, and particulates were well below the standards for waste incinerators.

Fate of Forgotten Fuel:
High-speed Laser-Induced Incandescence

Robbert Willems, r.c.willems@student.tue.nl
Peter-Christian Bakker, p.c.bakker@tue.nl
Nico Dam, n.j.dam@tue.nl

Eindhoven University of Technology

Conventional diesel combustion in compression ignition (CI) engines has become an established combustion technique by more than a century of dedicated research. Although such engines have superior efficiency over gasoline engines, they are plagued by harmful emissions of soot particles and nitrogen oxides (NO_x). Soot emissions have dropped more than an order of magnitude in the last decade, mainly due to improved fuel injection equipment and complex after-treatment systems. However, formation and oxidation processes, as well as radiative heat losses and their impact on engine efficiency, are still not well understood.

This work aims to qualitatively measure the in-cylinder soot processes on an optically-accessible CI engine using the well-established Laser-Induced Incandescence (LII) technique, albeit at high-repetition rate. The intention is to study the relatively unknown late-burn phase, i.e. after the injection has ended. Phase-averaged data does not provide all information here, because of the turbulent nature of the diesel combustion process. Measurement repetition rates in the order of several kilohertz enable the acquisition of crank-angle resolved data within a single combustion cycle. Ultimately, finding ways to speed up this late-phase combustion might be the key to improve engine efficiency and to reduce the emission of soot.

Applying a multi-kHz system gives rise to several challenges, such as step-wise sublimation or changes in morphology, since soot particles possibly experience multiple laser pulses. Additionally, retrieving information on soot volume fraction tends to be more difficult in engines because of changing ambient temperatures and increased conduction rates. Solutions for reducing the above mentioned effects are often contradicting, which further complicates experimental procedures.

Measurements on an atmospheric co-flow burner were done prior to engine experiments in order to identify possible problems with step-wise sublimation and other multiple exposure effects. It was found that, in this type of flame, a fluence around 0.1 J/cm^2 gives the best balance between the signal-to-background ratio, soot sublimation and local gas heating. This fluence, however, is well below the plateau regime of LII which creates additional problems with the interpretation of the signal when large temperature and density gradients, as well as a high degree of turbulence are present.

The many pitfalls with (high-speed) LII and the strategy to tackle these problems are discussed, and eventually some qualitative results are shown. The technique is considered feasible for qualitative measurements, but the balance between fluence, signal detection and changes to soot particle size and morphology was shown to be extremely delicate.

Two-dimensional electric fields in methane-air flames on the Heat Flux Burner

N. Speelman[a,*], N. Beishuizen[b], J.A. van Oijen[a]

[a] Department of Mechanical Engineering, Eindhoven University of Technology, The Netherlands
[b] Bosch Thermotechniek B.V., Deventer, The Netherlands

Introduction

In most combustion processes elementary reactions take place that produce electrically charged species and these charged species can have quite a pronounced effect on flame properties. Generally an electric field is applied to the flame and the movement of the reaction zone as a function of the applied electric field is studied. This effect has been studied extensively by numerous researchers, both experimentally (Fialkov [1997]; Goodings et al. [1979a,b]; Wortberg [1965]) and numerically (Belhi et al. [2010]; Cancian et al. [2013]; Jones et al. [1972]; Prager et al. [2007]).

These studies are primarily focussed on the concentration of charged species (Cancian et al. [2013]; Goodings et al. [1979a,b]; Jones et al. [1972]; Wortberg [1965]), or the effect of the electric field on flame stability and stand-off distance to the burner deck (Belhi et al. [2010]; Prager et al. [2007]). Fialkov [1997] gives a rather complete overview of the available literature and experimental work in the field.

Recently a physical and numerical model was developed at Eindhoven University of Technology to predict the electric currents that are encountered in flat methane-air flames (Speelman et al. [2015a,b]). This model qualitatively predicts the electric currents that were found by Peerlings et al. [2013]. The model is used to adapt the chemical mechanism and the transport properties in order to improve the numerical predictions made by the model. The draw-back of this model is that is only viable for flat flames.

The aim of this study is to extend the flat flame model to a model that is suitable to investigate the effect of electrode and burner geometries, because preliminary studies indicate that geometrical effects can have a significant effect on the electric field and as such on the electric current.

Multi-dimensional model

The model couples the Flamelet-Generated Manifold technique van Oijen and de Goey [2000] to the ANSYS® Fluent, Release 14.5.7 CFD solver. Two controlling variables are chosen to represent the flame behavior. The primary controlling variable is chosen to be the reaction progress variable CO_2 and the second controlling variable is the enthalpy to model the heat loss to the burner deck, because this important in the operation of the Heat Flux Burner Bosschaart [2002].

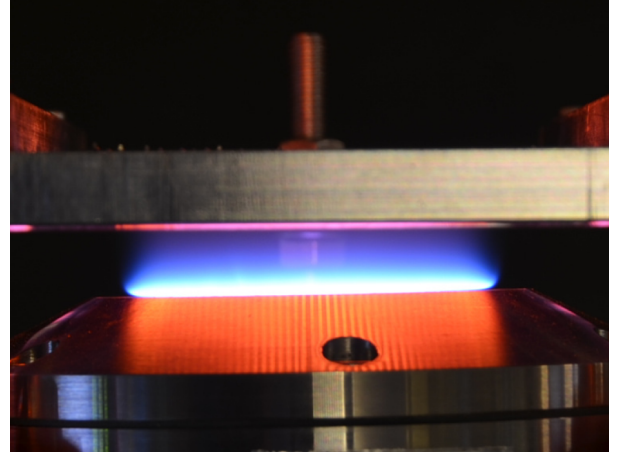* Corresponding author: N.Speelman@tue.nl

Figure 1: Experimental set-up with electrodes and flame.

To model the behavior of the electric field and the charged species in the flow a set of three coupled equations is added to the model. The first is Poisson's equation for the electric potential, given by (Lieberman and Lichtenberg [1994])

$$\vec{\nabla}^2 \Phi = -\vec{\nabla} \cdot \mathbf{E} = -\frac{q}{\varepsilon_0}, \qquad (1)$$

where Φ represents the electric potential, $\mathbf{E}$ is the electric field strength and the charge density is given by q. The behavior of the electrons and ions is modeled using a transport equation which includes electric diffusion. This is represented by

$$\frac{\partial \rho Y_i}{\partial t} + \vec{\nabla} \cdot (\rho Y_i \mathbf{v}) + \vec{\nabla} \cdot (S_i \rho \mu_i Y_i \mathbf{E}) - \vec{\nabla} \cdot \left(\frac{\lambda}{Le_i c_p} \vec{\nabla} Y_i \right) = \dot{\omega}_i, \qquad (2)$$

where S_i represents the charge number (1 for ions and -1 for electrons) of species i, μ_i represents the species electric mobility. In figure 2 it can be observed that this electric mobility is independent of the applied electric field and as such they are stored in the manifold.

In equation 2, $\dot{\omega}_i$ is the charged species source term, which is stored represented by a production and a consumption term. The production term is stored in the manifold, because it is independent of the applied electric field (Green and Sugden [1963]) and the consumption term is computed from the chemical source term accompanying the recombination reaction, given by

$$H_3O^+ + e^- \rightleftharpoons H_2O + H. \qquad (C.1)$$

Figure 2: Electric mobility of electrons.

Figure 4: Preliminary simulation of electric field strength for different electrodes.
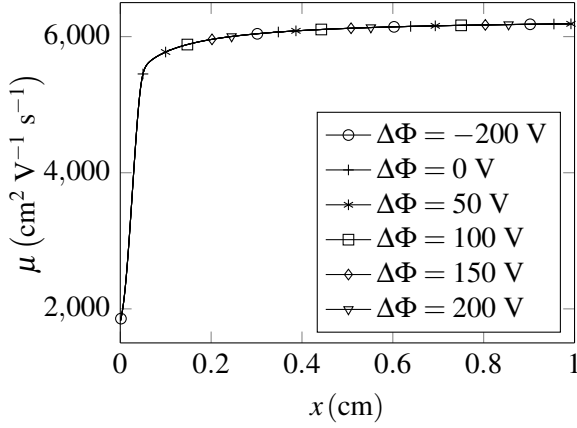
Finally the electric current is computed in a post-processing step from

$$\mathbf{J} = \sum_{i=1}^{N_S} q_i \left(\mathbf{v} + \mathbf{V}_i \right), \tag{3}$$

where N_S represents the number of charged species and $\mathbf{V}_i$ is the diffusion velocity of species i.

Validation set-up

To study the results of the numerical model, experimental work performed by Bosch Thermotechnology and at Eindhoven University of Technology is performed with a premixed burner stabilized flame and a adiabatic flat flame. The Bosch experimental setup uses a McKenna burner and the TU/e setup uses a Heat Flux Burner. The setup is shown in figure 1. These set-ups have been simulated with the CHEM1D one-dimensional flame code for a range of externally applied voltages and a range of different equivalence ratio's in Speelman et al. [2015a,b].

downstream electrodes. The first electrode that has been studied is a flat electrode, as is used by Peerlings et al. [2013]. This electrode applies a quasi-one-dimensional electric field to the flat flame to ensure good comparibility with one-dimensional simulations.

The second electrode is a pin electrode that is placed over the centerline of the flame and geometric effects might play a role in this case as can be found from a comparison between the saturation potentials for the different electrodes (see figure 3). An a-priori simulation, which assumes the basic one-dimensional charged distribution also holds in for the different electrodes is displayed in figure 4 and this immediately shows a vast difference between the electric fields for the two different electrodes. For this reason, this will be investigated further in this research.
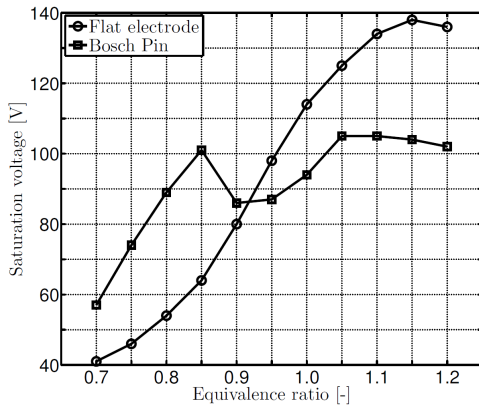
Acknowledgements

Figure 3: Comparison of saturation voltage for different electrodes (Source: Bruinsma [2015]).

The Heat Flux Burner set-up has also been investigated experimentally by Bruinsma [2015] for two different
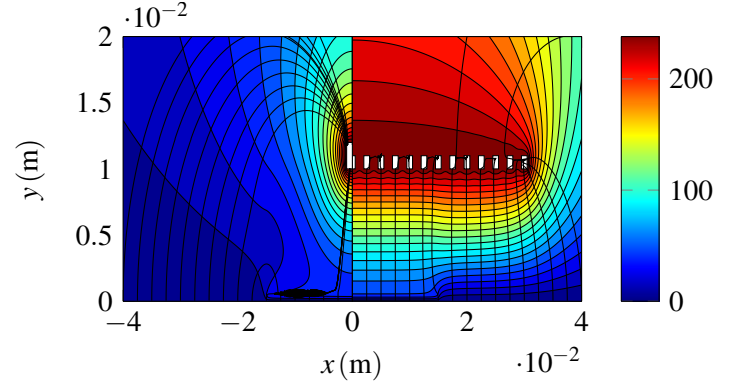
2

Effects of the mixture Lewis number on laminar flame stabilization and blow-off behavior

Yuriy Shoshin*, Rob Bastiaans, Philip De Goey

Eindhoven University of Technology, Eindhoven, NL

A wide use of hydrogen injection into the natural gas network is expected in Europe in the near future. The addition of hydrogen, produced using renewable or alternative energy sources, to natural gas, will contribute to reduce the emissions of greenhouse gases [1]. However, addition of hydrogen to methane can impact the flame stabilization behaviour due to specific effects related to the high mass diffusivity of hydrogen: so-called preferential diffusion effects. This may result in flashbacks, overheating and damage of gas appliance burners. Also unstable combustion and increase of pollutant emissions may occur. To adjust household appliances to fuel blends with variable content of hydrogen, new fuel-flexible burners have to be designed. To develop design rules for such burners, basic principles of the laminar flame stabilisation on solid obstacles have to be well understood. In modern boilers, perforated-plate stabilised premixed flame burners are commonly used. Flame stabilisation and blow-off mechanisms for such flames can be experimentally modelled by a laboratory inverted flame (which corresponds to small inter-hole distances on a perforated plate) and by a laminar bluff-body stabilised flame (corresponds to relatively large inter-hole spacing). Therefore, our research effort is focused on the experimental study of such flames for mixtures with varied fuel gas diffusivity.

Inverted flames were stabilised above the trailing edge of a thin rod installed along the centreline of a 12.5 mm ID glass tube. Rods of 1, 2, and 3 mm diameter were used in experiments [2]. In another set of experiments, flame was stabilised with cylindrical brass bluff bodies with 6x6 mm and 8x8 mm sizes. The cylinders were placed in a uniform mixture flow and supported from the bottom side by a 0.4 mm diameter steel rod. Plain propane, methane, and hydrogen-methane mixtures with varied hydrogen content were used as a fuel gas. Lean flame stabilisation limits have been determined for different fuel gases at varied fixed mixture approach velocities. Direct and Abel-inverted flame images were used to characterise the flame shape and, qualitatively, local burning rate variations along the flame. For inverted flames, heat fluxes to the flame holder have been determined using an infrared thermo-camera, and flow gas-dynamic structure in the flame anchoring region have been characterised using Particle Image Velocymetry (PIV) method.

For studied inverted- and bluff body-stabilised flames, a very strong influence of the fuel gas composition on flame stabilisation limits was found. Flames of mixtures with lower Lewis number (with higher fuel diffusivity, or, in the case of blended fuel, with higher hydrogen content) could be stabilised at lower equivalence ratios. Experimental blow-off velocities were plotted against burning velocities of 1-D zero-stretch flames, S_b, for corresponding mixtures. It was found that the values of S_b corresponding to the same flame blow-off velocity could differ several times for different fuel gases (Fig. 1). This is in contrast to a common view, used in burners' design, that S_b is the only parameter which determines the flame stabilisation behaviour [3].

Changing the fuel gas in a fuel-air mixture can even result in a qualitative change of the flame blow-off regime. Two "limit" blow-off regimes and transition between them have been observed in experiments even for the same flame holder and fixed mixture velocity (Fig. 2). In the first regime, corresponding to larger values of the mixture Lewis number (heavier fuel gas molecules), the whole flame was convected down-flow during the flame blow-off. In the second regime, corresponding to smaller Lewis numbers, a narrow neck appeared on the flame front above the vortex formed near a flame holder when flame stabilisation limit was approached. The flame blow-off occurred though the neck disruption in this case, similar to the blow-off regime found in numerical simulations for laminar bluff-body stabilised lean methane-air flame [4]. At higher mixture velocities and larger sizes of a flame

holder, the transition to the second regime occurred at higher mixtures Lewis number, and vice versa. For propane-air mixtures, however, only the first regime have been observed at all tested experimental conditions.
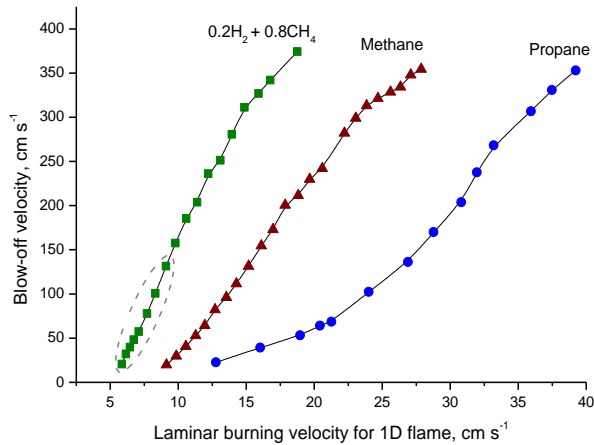

Fig. 1. Measured limits of stabilisation of inverted flame, plotted against adiabatic burning velocity for 1D flame.
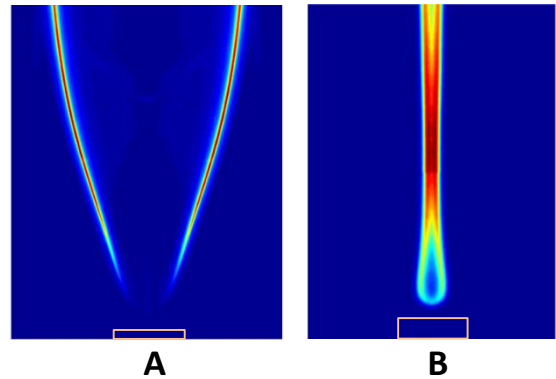

Fig. 2. Near-limit propane-air (**A**) and (0.2H2+0.8CH4)-air (**B**) flames stabilised above 8 mm dia. cylinder bluff body.

The maximum flame-stand-off distance measured at near-blow-off conditions was also found to depend on the fuel gas composition. It increased with the increase of the mixture Lewis number. For example, for inverted flames stabilised with 2 mm diameter rod, the maximum flame stand-off distance was ~ 2 mm for fuel the gas blend (0.2H2 + 0.8CH4) and ~ 6 mm for propane. At the same time, for a fixed fuel gas, this distance was almost unaffected by a 3-fold variation of the mixture velocity. Measurements of heat flux to the flame holder at the step-wise reduced mixture equivalence ratio showed that the bow-off always occurred at decreased, but still noticeable heat losses to the flame folder. This was observed even when the flame stand-off distance was much larger than the flame diffusion thickness, suggesting that heat was transferred from the flame base to the flame holder by convection. PIV measurements showed that, when flame was stabilised, a vortex is always present between the flame base and the flame holder. At large flame stand-off distances, the vortex is much longer than its size in the absence of the flame. The characteristic gas recirculation time in the vortex decreases when the blow-off limit is approached. When the flame stabilisation limit is reached, the vortex disrupts and shrinks down to its size in a cold mixture, and convection heat transfer between the flame and the flame holder interrupts. These observations evidence that heat transfer between the flame base and the flame holder plays a crucial role in inverted flames stabilisation.

To achieve detailed understanding of the observed phenomena, further investigations are planned, which will include PIV measurements and detailed simulations for laminar bluff-body stabilised flames.

References

1. R. Judd. Hydrogen blending and network adaptation. IEA Hydrogen Roadmap workshop June 10th 2013 Paris.
2. Y. Shoshyn, R.J.M. Bastiaans, L.P.H. de Goey. Anomalous blow-off behavior of laminar inverted flames of ultra-lean hydrogen-methane-air mixtures. Combustion and Flame, 160(3), 565-576, 2013.
3. B.K. Slim, H. Darmeveil, G.H.J. van Dijk, D. Last, G.T. Pieters, M.H. Rotink. , J.J. Overdiep, H.B. Levinsky. Should we add hydrogen to the natural gas grid to reduce co2-emissions? (consequences for gas utilization equipment). 23rd World Gas Conference, Amsterdam 2006
4. Kushal S. Kedia, Ahmed F. Ghoniem. The blow-off mechanism of a bluff-body stabilized laminar premixed flame. Combustion and Flame, 162 (4), 1304–1315, 2015.

Detailed simulation and flamelet modeling of laminar premixed flames interacting with cold walls

D. Mayer [a,*]   N. Beishuizen[b]   H. Pitsch[a]

[a] Institute for Combustion Technology, RWTH Aachen University, Aachen, Germany
[b] Bosch Thermotechniek B.V., Deventer, the Netherlands

Introduction Cooling processes in heat exchangers (HE) affect pollutant emissions of combustion devices. Moderate cooling in the post flame front region, where the bulk of CO conversion is close to completion but equilibrium is not reached yet, reduces the CO concentration downstream by favoring the exothermic CO to CO_2 oxidation. However, when the cooling is too strong or abrupt, e.g. when a flame impacts on a very cold wall, the oxidation of CO is interrupted, which leads to an excess of CO compared to adiabatic equilibrium. The desire for accurate predictions of these effects is obvious and ways to model them are necessary to reduce the computational costs.

Approach Using one and two dimensional (1D, 2D) detailed numerical simulations (DNS), we investigate the importance of CO-producing and CO-consuming elementary reactions in simplified HE geometries and analyze different ways to model the CO conversion in the framework of flamelet models in an a priori fashion. A two dimensional parameterization using the enthalpy and a chemical progress variable defined as the species mass fraction of CO_2 is used.

Geometry Three different geometries are available in which a HE is positioned with varying distance to the flame holder (see Fig. 1).
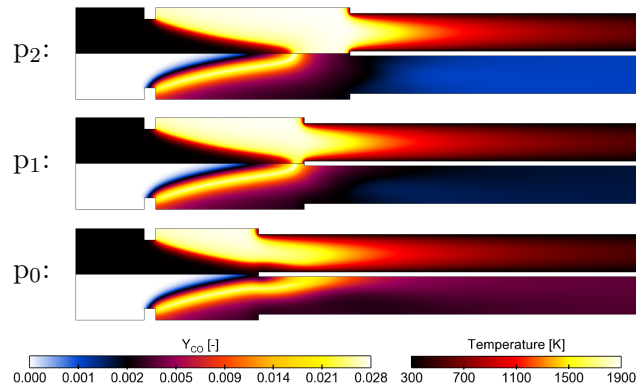

Figure 1: Computed temperature and CO mass fraction in simplified HE geometries.

In geometry p_2 the HE is positioned several flame thicknesses downstream of the flame front, while in p_1 the HE is very close to the flame tip, and in the case of p_0 the flame is penetrating the HE and hitting the cold walls.

Boundary conditions Simulations were performed with constant wall temperatures T_w from $1800\,\mathrm{K}$ to $300\,\mathrm{K}$ in equidistant steps of $300\,\mathrm{K}$. This enables to adjust the intensity of the cooling process and results in 18 different cases in total to analyze. The premixed gas is a methane-air mixture with an equivalence ratio of $\phi = 0.75$. The flow is laminar with a Reynolds number of $Re < 200$.

---

*Corresponding author. Email: d.mayer@itv.rwth-aachen.de

Techniques The simulations were performed using in-house codes [1, 2] and the GRI-Mech 2.11 [3] was applied. Differential diffusion was neglected and therefore the Lewis number was set to unity. A high resolution computational mesh was applied which resolves the temperature boundary layers and the flame front each with more than 15 computational cells.

Discussion The total mass reaction rate of CO can be calculated according to

$$\dot{\omega}_{CO} = \sum_{r=1}^{n_r} \dot{\omega}_{CO,r} = W_{CO} \sum_{r=1}^{n_r} \nu_{CO,r} \mathcal{Q}_r. \qquad (1)$$

Herein n_r is the number of elementary reactions, W_{CO} is the molecular weight of CO, $\nu_{CO,r}$ is the stoichiometric coefficient of CO in reaction r, and $\mathcal{Q}_r$ is the progress rate of reaction r [4].

To analyze the contributions of the individual elementary reactions to $\dot{\omega}_{CO}$, integral values of $\dot{\omega}_{CO,r}$ were investigated. As expected, it was found that elementary reaction (2) accounts for more than 99% of all negative CO mass reaction rates.

$$OH + CO \rightarrow H + CO_2 \qquad (2)$$

The progress rate for reaction (2) can be calculated according to

$$\mathcal{Q}_{(2)} = K_{(2)} \rho^2 \frac{Y_{CO}}{W_{CO}} \frac{Y_{OH}}{W_{OH}}, \qquad (3)$$

where $K_{(2)}$ is the kinetic rate of reaction (2), ρ the total density of the gas, and Y_i the mass fraction of species i [4]. For modeling CO emissions in a flamelet framework, this suggests to solve transport equations for Y_{CO} and Y_{OH}, and to use those mass fractions to correct the negative CO mass reaction rate $\dot{\omega}_{CO}^{-,lib}$ obtained from the flamelet library following

$$\dot{\omega}_{CO}^{corrected} = \dot{\omega}_{CO}^{+,lib} + \frac{\dot{\omega}_{CO}^{-,lib}}{Y_{CO}^{lib} Y_{OH}^{lib}} Y_{CO}^{trans} Y_{OH}^{trans}. \qquad (4)$$

Comparisons of CO mass reaction rates obtained from 2D DNS with uncorrected and corrected 1D DNS results, corrected using conditional mean values of Y_{CO} and Y_{OH} from the 2D DNS, show large improvements in all simulation cases with strong cooling. This is exemplarily presented in Figure 2 for geometry p_1 and $T_w = 900\,K$. It

shows the negative CO mass reaction rate $\dot{\omega}_{CO}^-$ conditioned on the median enthalpy interval $\tilde{h}$. The two 1D results of the same color represent solutions at enthalpy levels that limit the median enthalpy interval $\tilde{h}$.

The same analysis was applied to the mass reaction rate of OH. It is found that also for this rate a correction using the mass fraction of the OH radical improves the prediction accuracy. Further validation of the model is obtained by implementing the model in a commercial flow solver and performing simulations of the simplified HE configuration. A good improvement in the prediction of absolute values of the CO mass fraction and its trend is observed.
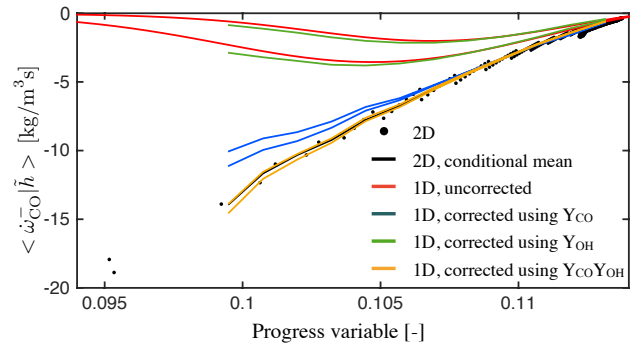
Figure 2: Comparison of 1D and 2D DNS results.

References

[1] O. Desjardins, G. Blanquart, G. Balarac, and H. Pitsch, "High order conservative finite difference scheme for variable density low Mach number turbulent flows," *Journal of Computational Physics*, vol. 227, pp. 7125–7159, July 2008.

[2] H. Pitsch, "FlameMaster: A C++ computer program for 0D combustion and 1D laminar flame calculations.," Last accessed September 18, 2015. http://www.itv.rwth-aachen.de/downloads/flamemaster/.

[3] C. T. Bowman, R. K. Hanson, D. F. Davidson, W. C. Gardiner, V. Lissianski, G. P. Smith, D. M. Golden, M. Frenklach, and M. Goldenberg, "GRI-MECH 2.11," Last accessed September 18, 2015. http://www.me.berkeley.edu/gri_mech/.

[4] T. Poinsot and D. Veynante, *Theoretical and Numerical Combustion*. Edwards, 2005.

Comparison of chemical mechanism, model flame and turbulence-chemistry interaction sub-models in FGM for Diesel combustion

C. Meijer and F.A. Tap* - *Dacolt International BV, Maastricht, NL*
L.M.T. Somers - *Eindhoven University of Technology, Eindhoven, NL*
Corresponding author: ferry.tap@dacolt.com

The Dacolt FGM combustion model is used as a tool for detailed CFD modeling of combustion processes. The Dacolt FGM combustion model has two main ingredients: (i) the FGM chemistry reduction technique [1] and (ii) presumed-PDF turbulence-chemistry interaction modelling. In this work two canonical configurations are used for the FGM model flame: the first consists of the ignition trajectory of homogenous reactors, while the second option is the use of counter flow diffusion flamelets with a presumed scalar dissipation rate. Turbulence-chemistry interaction is taken in to account through the variances for mixture fraction and/or progress variable. Flexibility with respect to chemical mechanism allows for the use of the LLNL C8-C16 n-Alkanes containing 1282 species [2], as well as the more common Luo mechanism with 105 species [3]. The computation of the model flames and post-processing is embedded in the Tabkin® software package of Dacolt [4]. The Dacolt FGM model is implemented in the OpenFOAM® CFD software environment [5], updated with a customized spray and mesh motion library [6].

Spray A – baseline validation

The ECN Spray A [7] case is used for basic validation as well as the numerical parameter study. The basic flame characteristics, such as ignition timing, flame lift-off length flame-structure are compared between the baseline case (homogeneous reactors, mixture fraction variance, Luo reaction mechanism) and experiments. The agreement for global characteristics like ignition timing and the flame stabilization position is very good, as presented in Table 1, for the case of 15 vol-% oxygen in the oxidizer. This confirms earlier findings for Spray H (n-heptane) [4] that the Dacolt FGM model is able to reproduce Diesel spray flame ignition and stabilization processes for low and high EGR levels.

Table 1: Flame ignition time and stabilization height

	Lift off length [mm]	Ignition delay [ms]
Experiment	16.5	0.44
CFD	17	0.45

Recent measurements with planar Laser-Induced Fluorescence of the OH radical [8] allow reconstructing the envelope of the reacting spray flame in a 2-dimensional plane. This measured flame structure is compared to the OH mass fraction extracted from the CFD simulation, shortly after ignition, between 0,6 and 0,8 ms, in Figure 1.
Although qualitative, the comparison illustrates that the Dacolt FGM model is able to quite closely reproduce the flame structure during the transient flame stabilization process. From the comparison it can be seen that the simulated flame seems to establish faster than in the measurement.

FGM sub-model variation

Three different FGM sub-models are varied in this study to assess their relative importance. Firstly, the reaction chemical mechanism is investigated. For global characteristics like ignition delay and flame lift-off, the differences are minor. For the mechanisms used this could be expected, as the reduced mechanism is based on the detailed mechanism. Using a mechanism from a different source shows more pronounced differences [9, 10]. Some differences are visible when looking at peak values of minor species like OH and CH2O. The flame structure, when plotted in mixture fraction space, remains quite similar.
Secondly, the effect of the turbulence-chemistry interaction (TCI) model is assessed. Without TCI, e.g. applying a δ-function as a presumed PDF, the peak values of temperature and species are higher and the turbulent diffusion flame front is visibly thinner. The application of a β-function as PDF over

mixture fraction or over mixture fraction and progress variable leads to a broader and more smooth flame structure in mixture fraction space. Peak values of temperature and species are reduced and the flame structure is widened.

Finally, a laminar diffusion flame is used as a chemistry sub-model, instead of the igniting Perfectly Stirred Reactor flame model. This leads to a more remarkable difference in flame structure, especially reducing the flame width in mixture fraction space through the effect of diffusion. Peak values of temperature and species around the stoichiometric point remain similar to the PSR values, especially when both are combined with a presumed β-PDF over mixture fraction. These observations are in line with previous findings [11, 12].
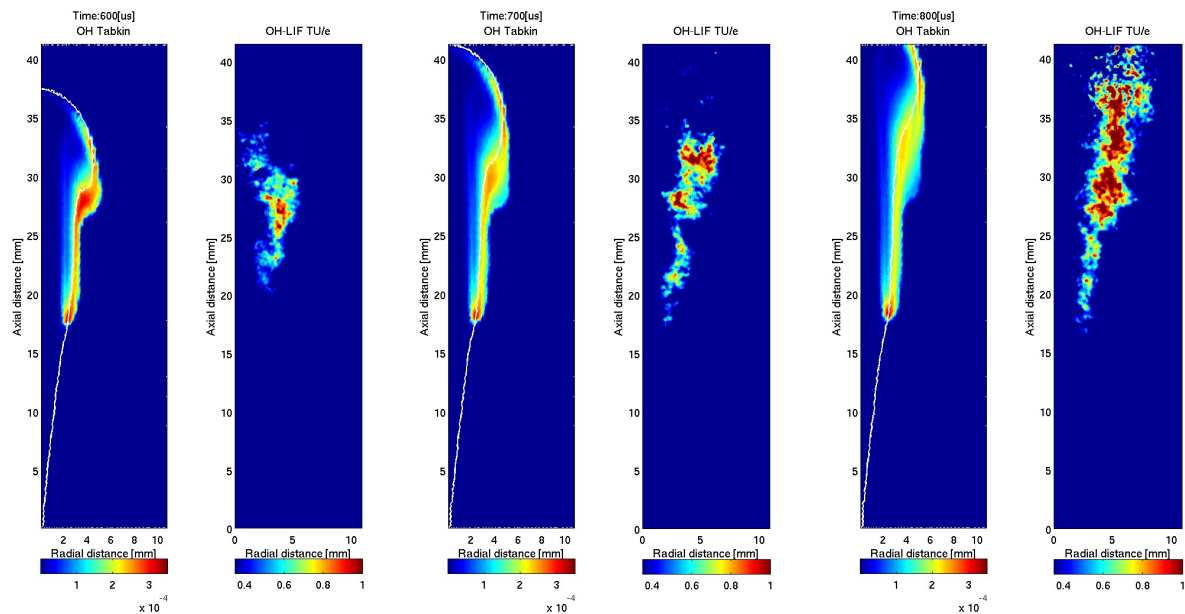

Figure 1: Comparison of flame structures at 0,6 | 0,7 | 0,8 ms after start of injection.

Conclusions and further work

The Dacolt FGM model implementation in OpenFOAM has been validated on both constant-volume Diesel spray flame and different sub-models are evaluated. The baseline results are encouraging, as the model is able to reproduce both the basic flame characteristics without any parameter tuning and with computation times below industry standards. Three sub-models of the FGM model were investigated: chemical mechanism, turbulence-chemistry interaction and model flamelet. Where the mechanism shows relatively minor effect on flame structure, the TCI model clearly broadens the flame brush and lowers peak values of temperature and species. Using a diffusion flamelet instead of a PSR yields a similar turbulent flame brush, but when plotted in mixture fraction space the flame is quite thinner through the diffusion effects, which are now captured. The difference in flame structure is presumed to have effects on especially CO and soot emission predictions, subject of further work.

References

1. J.A. van Oijen and L.P.H. de Goey, Combust. Sci. Technol. 161 (2000), pp. 113–137.
2. Westbrook, C. K. (2009). Combustion and Flame , 156 (1), 181-199.
3. Z. Luo et. al., Combustion and Theory Modeling, 18 (2) 187-203, 2014.
4. Tap, F. and Schapotschnikow, P., SAE Technical Paper 2012-01-0152.
5. OpenFOAM Foundation. http://www.openfoam.org, 2014.
6. Politecnico di Milano. Libice. http://www.engines.polimi.it/, 2014.
7. Engine Combustion Network. Ecn. http://www.sandia.gov/ecn/, 2014.
8. N.C.J. Maes. Characterisation of ECN "spray A" using optical diagnostics, TU/e, 2014.
9. A. Stagni, et al.,. *Industrial & Engineering Chemistry Research*, 2014.
10. C. Meijer. A detailed comparison of … Diesel Spray Combustion, TU/e, 2015
11. F.A. Tap and D. Veynante, Proc. Combust. Inst. 30:919-926 (2005).
12. C. Bekdemir et al., Proc. Combust. Inst. 3 34(2), 3067-3074 (2013).

TURBULENT COMBUSTION MODELING OF A CONFINED PREMIXED METHANE/AIR JET FLAME USING TABULATED CHEMISTRY INCLUDING HEAT LOSS FOR RANS AND LES

Simon Gövert
Jim B.W. Kok

Laboratory of Thermal Engineering, Faculty of Engineering Technology, University of Twente
Email: s.govert@utwente.nl

The present work addresses the coupling of a flamelet database, to a low-Mach approximation of the Navier-Stokes equations using scalar controlling variables. The model is characterized by the chemistry tabulation based on laminar premixed flamelets in combination with an optimal choice of the reaction progress variable, which is determined based on the computational singular perturbation (CSP) method. The current work focuses on turbulent premixed flames taking into account the effect of heat losses. The model is designed for applications in both, Reynolds-averaged Navier-Stokes (RANS) as well as large-eddy simulations (LES). A priori analysis of the database is presented to demonstrate the influence of the reaction progress definition. The validation of the turbulent case is performed using a turbulent premixed confined jet flame subject to strong heat losses, in which the model shows a good overall performance.

The presented combustion model makes use of the FPI/FGM approach for chemistry tabulation and is based on laminar premixed flamelets. Scalar controlling variables are used to couple the tabulated chemistry to the flow solver in the combustion simulation. In the current framework of premixed, non-adiabatic combustion, a thermo-chemical database is generated by systematically varying the conductive heat losses at the burner inlet using a burner stabilized premixed flame. The database is then parametrized in terms of the normalized enthalpy and the reaction progress variable (RPV), which represents the state of reaction, storing transport properties and the RPV source term.

While the RPV is usually defined based on heuristic approximations and a priori knowledge of the flame characteristics, an optimized choice of the RPV definition is proposed in the current work making use of the computational singular perturbation (CSP) method [1].

An approach based on presumed shape probability density functions (PDF) is applied for chemistry-turbulence interaction. The proposed model is applied to address high-fidelity numerical simulations in the context of large-eddy simulation (LES), but is also designed to provide acceptable results for industrial-type applications for Reynolds-averaged Navier-Stokes (RANS) simulations.

The proposed combustion model is implemented in the High-Performance Computing (HPC) multi-physics code Alya [2]. Alya is based on the Finite Element method and is designed for large-scale parallel applications.

The model is validated for the turbulent premixed jet flame that has been experimentally investigated by Lammel et al. [3] and the instantaneous temperature and velocity filed is presented in Figure 1.

The entire details about the numerical setup and the results can be found in [4].

REFERENCES

1. Massias, A., et al., *An algorithm for the construction of global reduced mechanisms with CSP data.* Combustion and Flame, 1999. **117**(4): p. 685-708.
2. BSC-CNS. *Alya multiphysics code*. 2014; Available from: http://www.bsc.es/computer-applications/alya-system.
3. Lammel, O., et al., *Experimental analysis of confined jet flames by laser measurement techniques.* J Eng Gas Turbines Power, 2012. **134**.
4. Gövert, S., et al., *Turbulent combustion modelling of a confined premixed jet flame including heat loss effects using tabulated chemistry.* Applied Energy, 2015. **156**: p. 804-815.
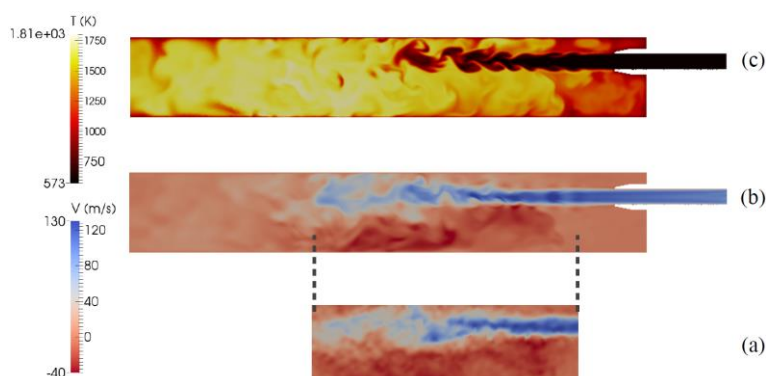
Figure 1: Instantaneous fields of axial velocity (a) experiments and (b) simulation; and temperature (c) simulation.

On the effect of LES sub-grid models for the opening angle of a swirling jet flow in a model gas-turbine combustor

W.J.S. Ramaekers and F.A. Tap* - *Dacolt International BV, Maastricht, NL*
B.J. Boersma - *Delft University of Technology, Delft, NL*
Corresponding author: ferry.tap@dacolt.com

Introduction

LES of gas turbine combustors is typically very demanding in terms of CPU-usage: small geometrical features and resolution of large turbulent eddies require fine numerical meshes, and small cells in high-velocity regions severely limit the numerical time step that can be used. Several open source codes for fluid flow simulations have been introduced, of which OpenFOAM is one of the most widely used ones. The primary goal of this study is to assess LES flow field predictions for the DLR gas turbine model combustor [1] using OpenFOAM® 2.2. Secondary, the effect of the Smagorinsky subgrid model for turbulent viscosity on the flow field predictions is investigated. This work build on previous work with URANS and DES [2] and confirms work by other groups that indicated a strong dependency of the flow field topology on the used LES subgrid model and mesh topology [3,4].

Model gas turbine combustor

The gas turbine model combustor investigated in this study is schematically depicted in Figure 1.

(a) Model combustor 3-D view
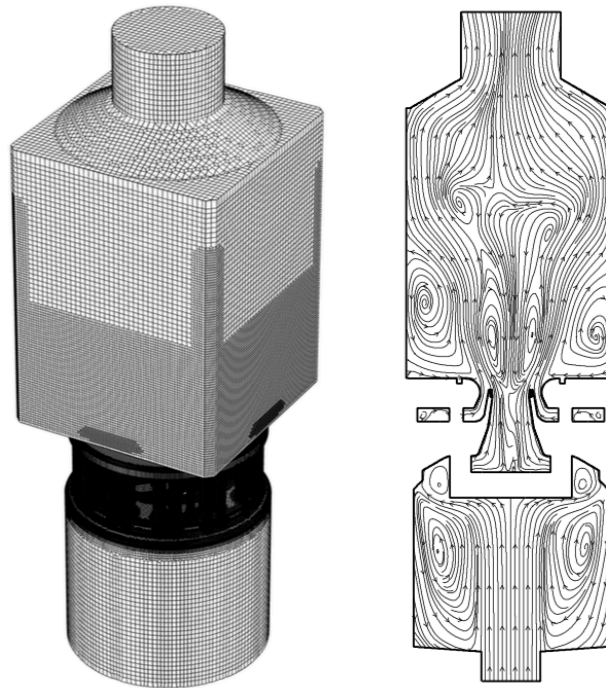
(b) Top view swirlers

(c) Bottom view swirlers
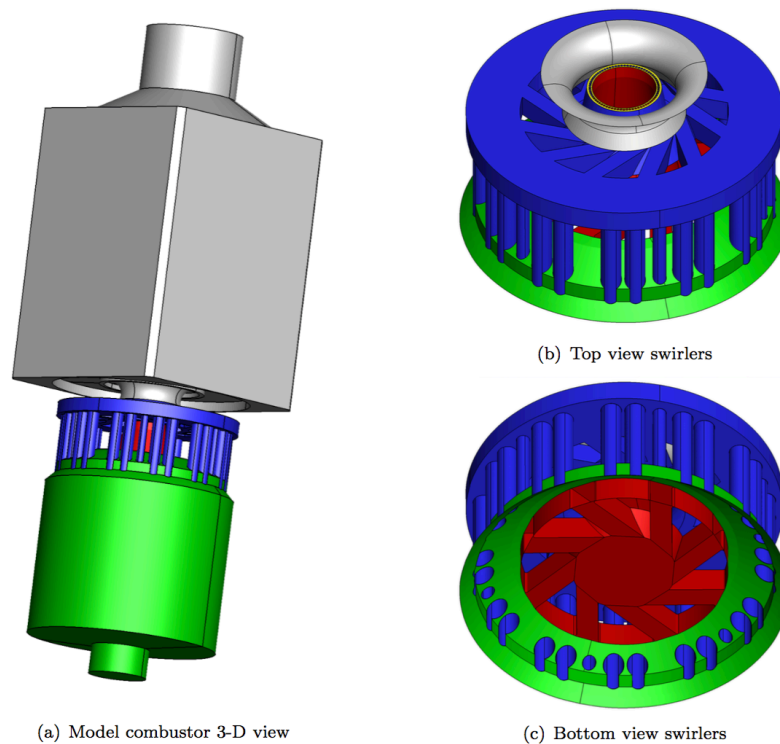
Figure 1: Gas turbine model combustor geometry

The air enters the plenum, depicted in green in figure 1(a). The air feeds into two concentric radial swirlers. The inner swirler is depicted in red in figure 1(c); it feeds to the combustion chamber through the central nozzle. The outer swirler (depicted in blue in figure 1(b)) is supplied with air from the plenum through twelve channels, and has a nozzle with a double-curved outer wall connected to the combustion chamber. Methane is injected into the combustion chamber through an annular ring of 72 small fuel tubes, depicted in yellow in the top view in figure 1(b). The combustion chamber has a square cross-section measuring 85 x 85 mm, and a height of 110 mm. All walls in the geometry are

treated as being adiabatic walls. The air plenum is included in this study, and assures a natural mass flow split between inner and outer swirler.

LES simulation set-up

The cold flow condition for Flame A from [1] is investigated. A hex-dominant mesh was used (Fig. 2), containing approx. 8.4 million cells with length scales ranging from approx. 0.03 mm in the fuel nozzles and on the double-curved nozzle wall, via approx. 0.5 mm in the swirlers and flame zone to approx. 4.0 mm in the downstream region of the combustion chamber.

LES simulation results

The measured flow field [1] is very well reproduced by the LES simulation. Figure 2 gives an impression of the flow field topology, showing the inner and outer recirculation zones. The effect of the Smagorinsky

Figure 2: left: computational mesh, right: typical flow pattern

contant is investigated in Figure 3. The black dot corresponds to the obtained opening angle using the standard Smagorinsky coefficient of 0.2, the red dot to the obtained opening angle using 75% of the standard value and the blue dot to the obtained opening angle using 50% of the standard value. These findings confirm the importance of LES subgrid modeling.
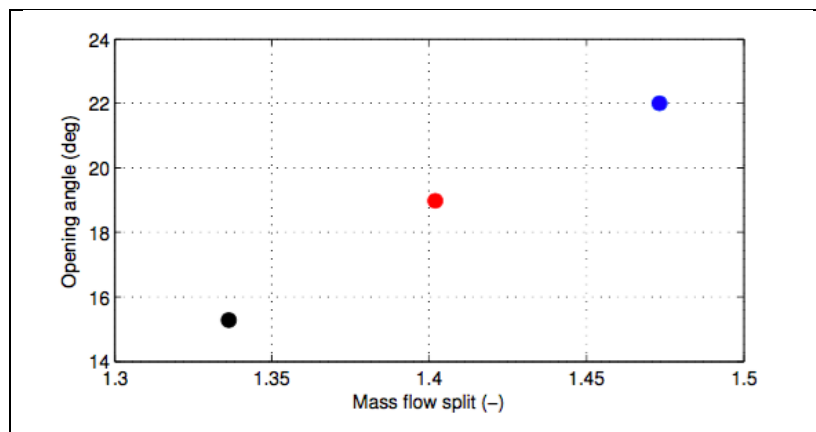
Figure 3: Effect of Smagorinsky contant on mass flow split

References

1. P. Weigand, W. Meier, X.R. Duan, W. Stricker and M. Aigner, Investigation of Swirl Flames in a Gas Turbine Model Combustor 1: Flow-field, structures, temperature and species distributions, Combust. Flame 144, pp. 205–224 (2006).
2. M. Wankhede, F. Tap, P. Schapotschnikow and W. Ramaekers, Numerical Study of Unsteady Flow- Field and Flame Dynamics in a Gas Turbine Model Combustor, GT2014-25784, Proc. ASME Turbo Expo 2014 (2014).
3. Y.C. See and M. Ihme, Large Eddy Simulation of a Gas Turbine Model Combustor, AIAA 2013-0172 (2013).
4. Y.C. See and M. Ihme, LES Investigation of Flow Field Sensitivity in a Gas Turbine Model Com- bustor, AIAA 2014-0621 (2014)

Still burning after all these years: better, cleaner, and less

Simone Hochgreb, University of Cambridge, Cambridge, UK

simone.hochgreb@eng.cam.ac.uk

Many of us growing up in the 70s and 80s might have dreamed of a future in the following century where we would have of jet-powered vehicles, in a world where energy needs have been solved, and environmental problems a thing of the past. Fast forward to today and we are perhaps disappointed to find that we have not yet solved all problems on that front, and continue to use evolutionary rather than revolutionary techniques. We can clearly see that our pathways for future solutions is largely driven by the existing technology base, and that the development of solutions is often driven by economic and regulatory demands. That largely explains why we are still burning more than ever, in spite of the perennial threat of peak oil, yet finding creative solutions inside the energy and combustion box remains ever more relevant if we are to survive into the next century.

In this talk we will review past and current progress and needs in experiments and modeling in turbulent combustion applied to continuous processes, such as powerplants and aeroengine gas turbines. We identify areas where predictions are robust, others we are still rather far from turnkey solutions, and some potential areas that may enable faster progress.

Experimental database on turbulent spray flames in hot-diluted coflow

H. Correia Rodrigues, M.J. Tummers, E.H. van Veen, D.J.E.M.Roekaerts*

Department Process and Energy, Delft University of Technology, The Netherlands
*d.j.e.m.roekaerts@tudelft.nl

Abstract: The Delft Spray in Hot Coflow (DSHC) database contains results of an experimental investigation of spray flames generated using a laboratory-scale burner [1-3] and is available for model validation studies. The flow configuration used consists of a spray jet injected into a coaxial upward flow of either air or combustion products from a secondary burner operating in lean conditions. The latter case resembles an environment with temperature and oxygen concentration typical for combustion in highly diluted air diluted (flameless combustion or MILD combustion). The spray is created using a commercial pressure-swirl atomizer. Ethanol and acetone were used as fuel. Flames with several combinations of spray and coflow conditions were studied in detail. Datasets are available for coflow of air and of lean combustion products with three different levels of O_2-concentration and for flames of ethanol and acetone at identical coflow conditions. Atomization mechanisms were revealed by high-speed camera observations. Complementary laser based diagnostic techniques, PDA and CARS were employed to characterize the properties of gas and liquid phase. PDA provided simultaneous measurements of droplet velocity and size statistics and CARS the gas-phase temperature statistics. The velocity and temperature statistics of the coflow were measured using respectively LDA and CARS. The composition of the coflow was measured using a flue gas analyzer. The poster gives an overview of the studied cases, the available data and the current insight on the flame structure.
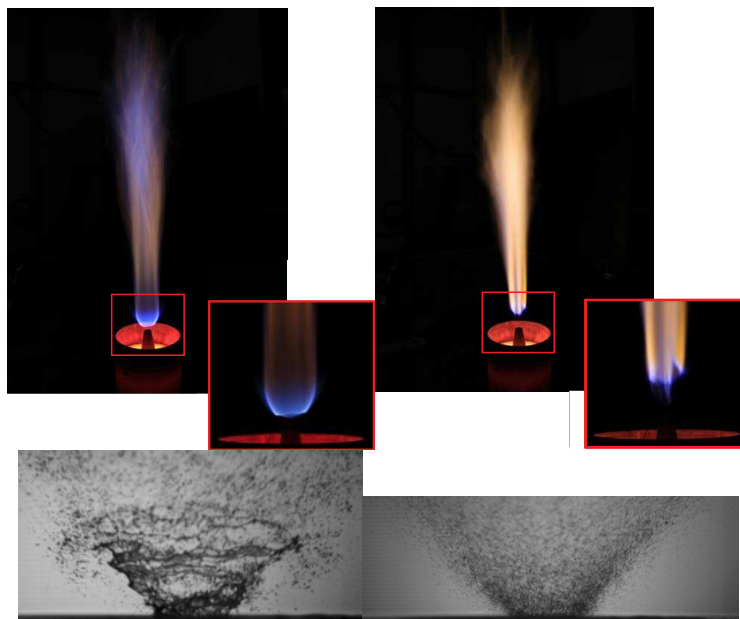
Figure 1:

References
1. H. Correia Rodrigues, M.J. Tummers, E.H. van Veen, D.J.E.M. Roekaerts, Combustion and Flame, 162 (2015) 759-773
2. H. Correia Rodrigues, M.J. Tummers, E.H. van Veen, D.J.E.M. Roekaerts, Int. J. Heat Fluid Flow, 51 (2015) pp. 309-323
3. H. Correia Rodrigues, Spray combustion in moderate and intense low-oxygen conditions. An experimental study, PhD Thesis, Delft University of Technology, 2015

Response of premixed counterflow flame to a heaviside strain rate

Akshay Iyer*, Jeroen van Oijen*, Jan ten Thije Boonkkamp**

September 16, 2015

* Department of Mechanical Engineering, Technische Universiteit Eindhoven.
** Department of Mathematics and Computer Science, Technische Universiteit Eindhoven.

Unsteady strain rates significantly change the flame characteristics and hence it is necessary to study these flame-flow interactions for laminar flames. In literature premixed counterflow flame with unsteady strain rates have been studied, but most of the unsteadiness are oscillatory in nature [1, 2]. One of the most fundamental ways of introducing unsteadiness in the applied strain is by introducing a step function[3]. A counterflow flame with a step function or heaviside applied strain rate will be subjected to unsteadiness at the strain application, but will reach a steady state with the progress of time. This initial unsteadiness caused by sudden change of strain will affect many key parameters such as massflow rate, flame motion, species diffusion etc before they attain a steady state. In this study we would like to investigate the flame's response to a heaviside strain rate in terms of massflow rate and flame motion and try to model the same using a 1$^{\text{st}}$ order approximated model. In order to avoid the complexity of preferential diffusion our test flame is a premixed methane-air unity-Lewis counterflow flame with $\phi = 0.8$, and subjected to an applied heaviside strain rate given by,

$$a_{\text{in}}(t) = \begin{cases} \bar{a} & \text{if } t \leq 0 \\ \bar{a} + \Delta a & \text{if } t > 0. \end{cases}$$

The simulation of the counterflow flame was done using the TU/e inhouse code CHEM1d, with DRM-19 chemcial mechanism. In fig. 1, the instantenous change in strain rate and massflow rate at different time instances are plotted and it can be clearly seen that for positive heaviside strain the strain profile and the massflow profile is different from the steady state profile at $t = 0^+$, and takes a finite time to reach it. For a negative heaviside strain, the instantaneous strain rate has steep negative gradient, and the mass flow is negative at $t = 0^+$.Hence it becomes important to study the flame position of such a counterflow flame through which we will be able to judge the flame's ability to adapt to a changing strain rate. This will allow us to study the flame's reaction time to changes in applied strain, and will through light into time-scales associated with an unsteady counterflow flame, and its coupling with flow straining.

The flame takes a finite time to respond to rapidly changing applied strain and the response time of the flame is dependent on $\bar{a}$, Δa, and also flame time-
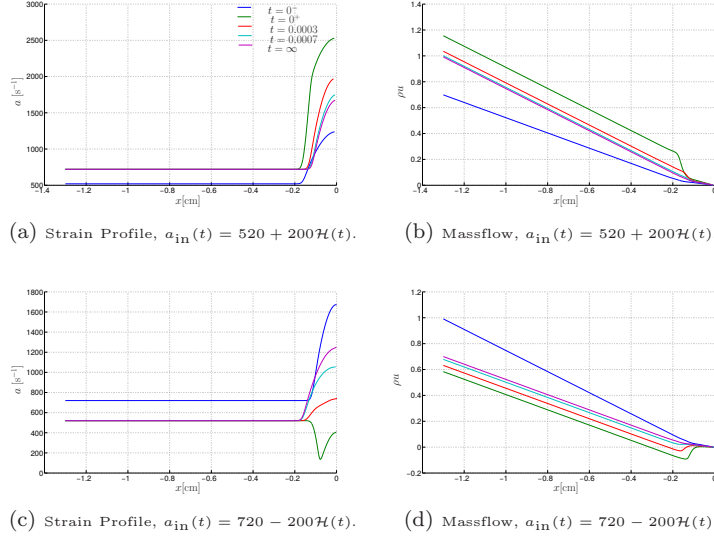
(a) Strain Profile, $a_{\text{in}}(t) = 520 + 200\mathcal{H}(t)$.

(b) Massflow, $a_{\text{in}}(t) = 520 + 200\mathcal{H}(t)$.

(c) Strain Profile, $a_{\text{in}}(t) = 720 - 200\mathcal{H}(t)$.

(d) Massflow, $a_{\text{in}}(t) = 720 - 200\mathcal{H}(t)$.

Figure 1: Spatial profiles of strain and massflow in time of counterflow flame with $a_{\text{in}} = 520 + 200(H)(t)$ and $a_{\text{in}} = 720 - 200(H)(t)$.

scales. It was seen that the premixed flame is able to handle instanteous strain rates which are higher than the extinction strain rate and also instanteous negative strain rate. The motion of the flame position when subjected to a negative heaviside strain jump has second order effects as the massflow is instanteously negative. With the help of the flame reaction time it will be easy to define high and low frequency regimes for an oscillating counterflow flame. The flame position modelling done using a first order model is able to predict the flame response time trends, though it fails to capture second order effects and doesnt predict the steady state flame position accurately.

References

[1] Z. Huang, J. K. Bechtold, and M. Matalon (1998), *Weakly stretched premixed flame in oscillating flows*, Combust. Theory Modelling , 2:115-133.

[2] H.G. Im , J.K. Bechtold, and C.K. Law (1996), *Response of counterflow premixed flame to oscillating strain rates*, Combust. flame, 105:358-372.

[3] T. Poinsot, D. Veynante *Theoretical and Numerical Combustion*, 2$^{\text{nd}}$ Edition, Edwards Publication.

The effect of the perforation geometry of plate burners on flame stability - Experimental and numerical approach

S. Kruse [a,*]   D. Mayer[a]   P. Milz[a]   N. Beishuizen[b]   H. Pitsch[a]

[a] Institute for Combustion Technology, RWTH Aachen University, Aachen, Germany
[b] Bosch Thermotechniek B.V., Deventer, the Netherlands

Introduction   Porous media or perforated plates are widely used for flame stabilization in compact household gas burners [1]. Their design has a major effect on burner efficiency and emissions. While the flame holder enables a stable flame, heat losses of the flame to the burner plate result in lower burner efficiencies, and for lower power stages also, in flame extinction causing increased carbon monoxide (CO) and unburnt hydrocarbon (uHC) emissions. In order to understand the dependence of the plate design on the combustion stability, especially for low power operation, different plate perforation geometries are experimentally and numerically investigated. Therefore, stability tests for flame extinction at low power operation points are performed. Also, flame temperatures and flame position are determined with optical diagnostics. These data are used to validate detailed simulations and simulations based on a flamelet progress variable (FPV) approach, which both consider the conjugate heat transfer in the perforated plate.

Experimental setup   In this study, a laminar premixed burner is used. Fuel (CH_4) and air are injected separately at the burner bottom. An internal mixing device, as well as the mixing distance of about $l/d = 5$ between burner in- and outlet ensure a homogeneous CH_4-air mixture at the exit. The power and equivalence ratio are adjusted by controlling the fuel and air flow using laminar flow element mass flow controllers. The burner outlet diameter is 55 mm and features the possibility to mount different perforated plates at the exit.

As a reference case to compare experimental and numerical results, a plate with nine rectangular slots offering two-dimensional symmetry is used. Afterwards, several plates differing in blocking ratio, hole diameter, and hole separation distance are investigated and their effect on flame stability is analyzed. The plate temperatures are determined by thermocouples welded at several locations on each plate.
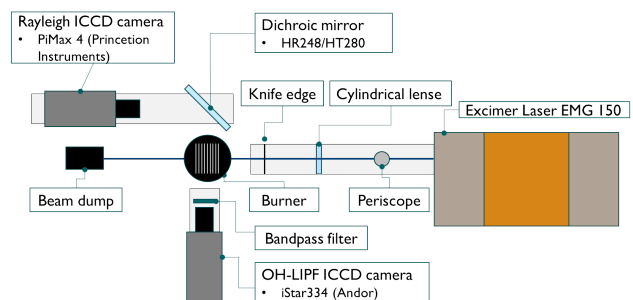

Figure 1: Experimental and diagnostic setup

In order to provide detailed, simultaneous in-

*Corresponding author. Email: s.kruse@itv.rwth-aachen.de

1

formation of flame position and temperature, Rayleigh combined with OH-Laser Induced Predissociation Fluorescence (LIPF) is applied to the premixed flame. While the Rayleigh signal indicates the local temperature, the position of the reaction zone is determined by the OH-LIPF signal [2]. A tunable Excimer laser serves as a light source. The light sheet is focused above the burner. Rayleigh and OH-LIPF signals are simultaneously detected by two intensified CCD cameras. Details of the optical setup are shown in Fig. 1.

Numerical setup Detailed simulations are performed using an in-house code [3] and the GRI-MECH 2.11 mechanism [4]. The grid resolution resolves the flame front and the temperature boundary layer each with more than 10 cells.

To accurately predict the wall temperature dependent flame stabilization, conjugate heat transfer in the solid is accounted for by solving an energy equation in the solid. The temperature fields are coupled at the fluid/solid interface [5]. At the fluid side, the temperature is prescribed using a Dirichlet boundary conditions and at the solid side a Neumann boundary condition is imposed. The time step used for solving the energy equation in the solid is increased by a constant factor to achieve faster convergence of steady state problems.

For the FPV model, a parametrization using the mass fraction of CO_2 and the enthalpy is used. Detailed information on the FPV model can be found in [6]. The chemistry table used for the FPV simulations was compiled using 1D unstretched premixed flame simulations computed using the FlameMaster code [7].

Approach and Outlook In order to analyze the effect of the perforation geometry on flame stabilization, an experimental stability analysis is performed for several perforated plates. The output power is gradually reduced until flame extinction occurs. For the analysis, the power at flame extinction is related to the ratio of nozzle diameter, nozzle separation distance, as well as the burner exit velocity. In order to provide more detailed information on flame location and temperature distribution, optical investigations are performed.

In a first step, data to validate the numerical setup is generated using a geometrically simple perforation. To gain deeper insight into the effect of the perforation geometry on the flame heights and the temperature distribution, different perforation geometries and selected load points are investigated.

For numerical model validation, experimental measurements of the slot plate are used. The simulations of the slot plate are performed in a two-dimensional setup using symmetry conditions. After validation, the FPV model is used for three-dimensional simulations of more complex plate geometries and for the design of novel burner geometries.

The combined numerical and experimental approach supports the development of new optimized perforation geometries to increase the efficiency and lower emissions of household burners in a wide operation power range.

References

[1] K. Kedia and A. Ghoniem *Proc. Combust. Inst.*, vol. 34, pp. 921–928, 2013.

[2] P. Andresen, A. Bath, and W. Grger *Appl. Optics*, vol. 27, pp. 365–378, 1988.

[3] O. Desjardins, G. Blanquart, G. Balarac, and H. Pitsch *Journal of Computational Physics*, vol. 227, pp. 7125–7159, July 2008.

[4] C. T. Bowman, R. K. Hanson, D. F. Davidson, W. C. Gardiner, V. Lissianski, G. P. Smith, D. M. Golden, M. Frenklach, and M. Goldenberg, "GRI-MECH 2.11," Last accessed September 18, 2015. http://www.me.berkeley.edu/gri_mech/.

[5] V. Kazemi-Kamyab, A. van Zuijlen, and H. Bijl *J. Comput. Phys.*, vol. 272, no. 0, pp. 471 – 486, 2014.

[6] C. D. Pierce and P. Moin *J. Fluid. Mech.*, vol. 504, pp. 317–347, 2005.

[7] H. Pitsch, "FlameMaster: A C++ computer program for 0D combustion and 1D laminar flame calculations.," Last accessed September 18, 2015. http://www.itv.rwth-aachen.de/downloads/flamemaster/.

Determination of the fractal dimension of silica aggregates in 1-D methane/hexamethyldisiloxane/air flames by light scattering measurements

P.N. Langenkamp[1], H.B. Levinsky[1,2], A.V. Mokhov[1]

[1]*Combustion Technology, Energy and Sustainability Research Institute, University of Groningen, Nijenborgh 4, 9747 AG Groningen, The Netherlands*
[2]*DNV GL - Oil & Gas, Nederland B. V. – P.O. Box 2029, 9704 CA Groningen, The Netherlands*

Biogases can play an important role in a (partial) transition away from fossil fuels, but often contain impurities such as siloxanes. SiO_2 molecules generated in the combustion of the siloxanes coalesce together into particles which subsequently form even larger aggregates and deposit on internal parts of combustion equipment. We used angle dependent light scattering as a quicker and less invasive alternative to ex-situ methods such as TEM to investigate aggregate growth in premixed CH_4/hexamethyldisoloxane (L2)/air flames as a function of residence time.

L2 was added to burner stabilized premixed methane/air flames through a bubbler system (Fig. 1.). The flame temperature is controlled by changing exit velocities of the total gas mixture and determined by solving the governing equations with Cantera suite code using the GRI-Mech 3.0 chemical mechanism. A 532 nm laser is directed through the flames. The scattered light is detected by photomultipliers placed at four distinct angles. Calibration of the measured signals was performed using Rayleigh scattering from SF_6.

The angle dependence of the scattered signal can be used to determine the mass-averaged root-mean-square radius (radius of gyration) R_g of the aggregates. From the dependence of the absolute scattered signal on R_g we can subsequently get an estimate of the fractal dimension D_f – a measure of how the number of primary particles that make up an aggregate scales
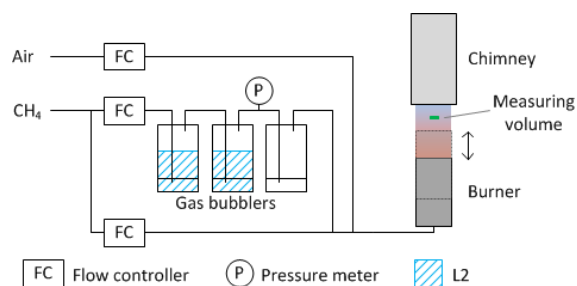

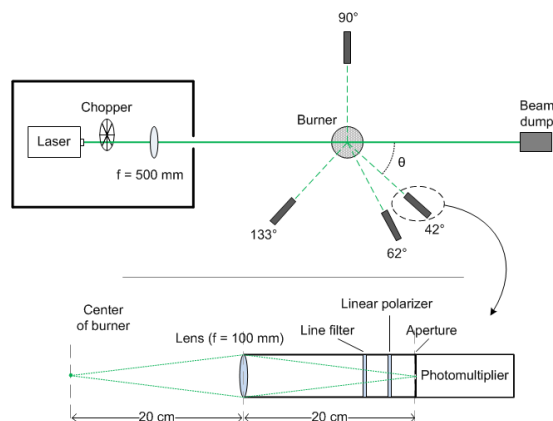Fig. 1. Height adjustable burner system and gas supply with bubbler system to seed the flame with L2

Fig. 2. Schematic of the light scattering setup. The angular orientations of the collection systems are with respect to the forward direction of the laser beam.

with the aggregate's radius of gyration [1]:

$$n = \left(\frac{R_g}{a}\right)^{D_f}$$

where a is the radius of the (assumed to be spherical) primary particles.

Fig. 3. shows the radii measured in stoichiometric flames at 1950 K for a range of silica concentrations. We observe a less-than-linear dependence of R_g on height above the burner (which is proportional to the aggregate's residence time). The smallest measured R_g is approximately 15 nm as the fitting procedure used to determine R_g yielded unreliable results at heights where we expect even smaller R_g. The fractal dimension of silica aggregates as function of silica concentration, determined for the same data set, is presented in Fig. 4. Estimated values for D_f of 2.0 to 2.3 exceed typical values reported in literature of 1.75 to 1.9 [2]. This can be attributed to primary particle growth inside fractal aggregates, that was neglected in our estimation of D_f.
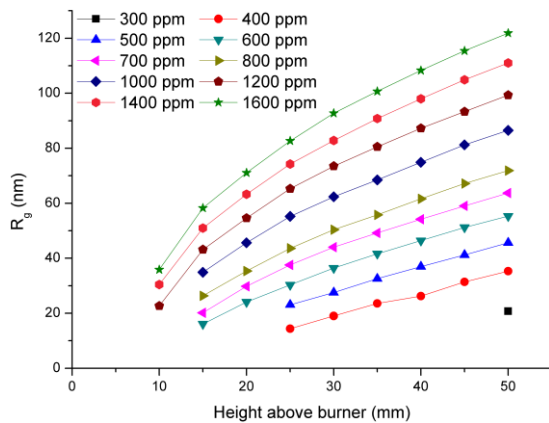

Fig. 3. R_g for 1950 K stoichiometric flames containing various amounts of silica, as a function of height above the burner.
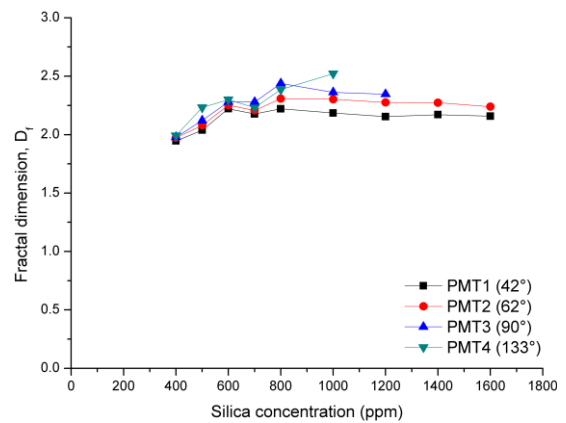
Fig. 4. Fractal dimension as function of siloxane concentration, as determined at four separate angles.

[1]   B. B. Mandelbrot, *The Fractal Geometry of Nature*. New York: W.H. Freeman and Co., 1982.

[2]   C. M. Sorensen, "Light Scattering by Fractal Aggregates : A Review," *Aerosol Sci. Technol.*, vol. 35, no. 2, pp. 648–687, 2001.

Large Eddy Simulation of MILD spray jet flames

L. Ma, D.J.E.M. Roekaerts

l.ma@tudelft.nl

Department of Process and Energy, Delft University of Technology, the Netherlands

Abstract

The influence of coflow conditions on the structure of the Delft Spray in Hot-diluted Coflow (DSHC) flames was studied using Large Eddy Simulation (LES) technique. The developed modeling approach was first applied to three different experimental cases for validation. Major properties like droplet velocity, SMD, gas phase velocity and temperature can be reproduced with good accuracy. Also, the trends of flame lift-off height and flame width with change of coflow conditions were properly captured. Then the study was extended to four more virtual cases, which differ from each other only by coflow temperature or O_2 concentration. The purpose of this step is to eliminate the simultaneous change of multi-parameters in experiment and to isolate the influences of coflow temperature and O_2 concentration, which are important parameters for a MILD furnace design and operation. Two reaction regions (RRs) have been identified to exist in the DSHC flame. The inner RR is created by the premixed reaction of C_2H_5OH under hot and fuel rich condition. The outer one is formed by the non-premixed reaction of intermediate fuels, e.g. CO and H_2, which are produced in the inner RR. The coflow temperature (T_{cf}) has a significant influence on the DSHC flames. Five times increase of flame lift-off height was observed when the coflow temperature was decreased from 1400 K to 1200 K. The flame changed from two-RRs structure to a triple flame when the coflow temperature is reduced. The outer RR shifted from non-premixed combustion at high T_{cf} to premixed combustion at low T_{cf}. The O_2 concentration in the coflow ($X_{O2,cf}$) alters the role of two RRs. The inner premixed RR is strengthened with increasing $X_{O2,cf}$. The flame peak temperature is significantly increased in the case with highest $X_{O2,cf}$. All cases except the one that has the highest $X_{O2,cf}$, falls into the MILD regime according to the definition based on maximum temperature increase. But when the restriction of flame peak temperature ($T_{peak} < 1800$ K) is also applied, only the case with the lowest $X_{O2,cf}$ can be strictly called MILD.

Heavy-Duty Diesel Spray in a High-Pressure, High-Temperature Vessel: Towards Spray-Wall Interaction

N.C.J. Maes[a,*], N.J. Dam[a], L.M.T. Somers[a], G. Hardy[b]

[a]*Department of Mechanical Engineering, Eindhoven University of Technology, P.O. Box 513, 5600 MB Eindhoven, The Netherlands*
[b]*FPT Motorenforschung AG, Schlossgasse 2, CH-9320, Arbon, Switzerland*
[*]*Corresponding author: Noud Maes (n.c.j.maes@tue.nl)*

Motivation

The contemporary choice for the propulsion of most transport and agriculture applications still features a rather classical heavy-duty Diesel engine. This well-developed concept for propulsion, has been under continues development for more than a century now. The immense success of the Diesel engine is found in the advantages of both power and load capability while maintaining high efficiency. Therefore, it is expected that the Diesel engine will dominate the transport and agriculture market for at least a number of decades to come. However, the increasing demand for a reduction in emissions and fuel consumption by legislation and customers points out the necessity of further research to improve the current generation of Diesel engines.

Key to the improvement of the modern Diesel engines, is a detailed understanding of combustion at relevant conditions for these applications. Although many studies focus on reacting fuel sprays at pressures around or below 60 bar, there is a definite need for much higher values. By generating relevant and accurate data at well-defined boundary conditions in a dedicated test-rig, fuel sprays can be characterized in a detailed manner, creating the possibility to study important parameters in great detail. The obtained data can subsequently be used to validate and calibrate numerical simulations. The influence of specific parameters, combustion, and an obstructing wall will be studied individually by adjusting or adding them in a systematic way. Using the combined strength of experiments and high-fidelity models will provide a constructive understanding of Diesel combustion, aimed at a significant step toward the demanded improvements.
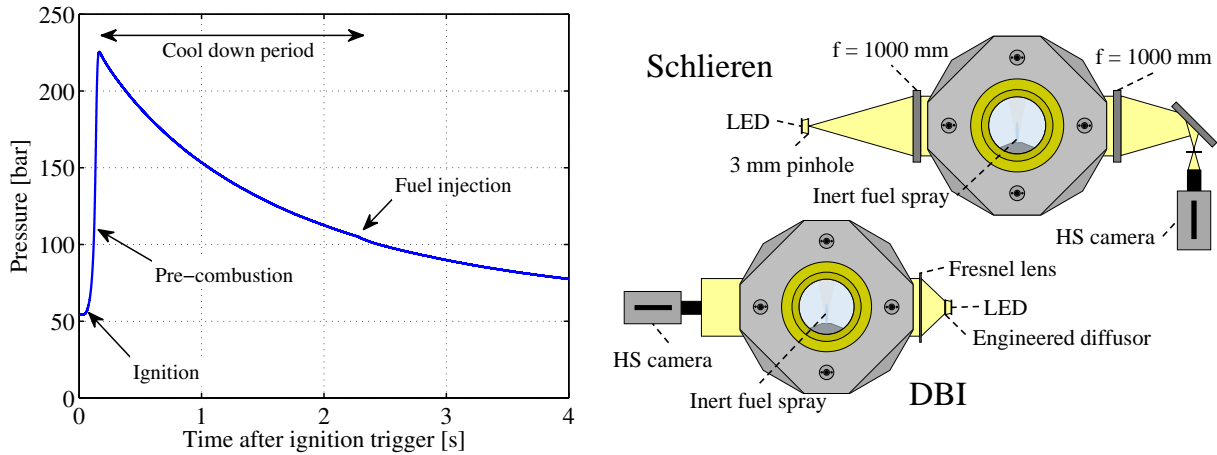

Figure 1: Left: pressure in the vessel during a typical experiment, showing main events and their time scales. After the pre-combustion, there is no oxygen left, thus the injection is only visible by a small decrease in pressure due to evaporative cooling. Right: illustration of the setup with two diagnostic techniques used in this work. Additional explanation of the diagnostic techniques is provided in the text.

Experimental setup

The Eindhoven High Pressure Cell (EHPC) is an optically accessible, constant volume vessel which is designed to study fuel sprays at engine-like conditions [1]. In order to achieve these conditions, the vessel is pre-heated and filled with a so-called pre-burn mixture. Upon spark ignition of the pre-burn mixture, the temperature and pressure in the vessel rapidly increases. During the relatively long cool-down period, governed by heat losses to the walls, desired conditions will be met and the fuel is injected. The pressure during an experiment is depicted in the left image of Figure 1. The conditions in this work have been chosen such that they are relevant to the current heavy-duty Diesel engines at top dead center, having an ambient temperature of 900 K, a density of 40 kg/m^3 and an injection pressure of 800 bar. Simultaneously, the conditions were chosen to match a different, already existing database to which contributions have been made in the past [2]. The most significant difference with these previous experiments, is a nearly double ambient density, resulting in much higher pressure inside the vessel. The fuel injector for these experiments features a custom-made, single orifice with a diameter of 205 μm.

Optical diagnostic techniques

Two different high-speed (160 kHz) diagnostic techniques have been used to visualize the evaporating fuel sprays in this study. The right image in Figure 1 illustrates the optical setups with relevant components. The upper arrangement depends on the detection of non-refracted light-rays to visualize changes in density. This technique therefore captures the entire spray, independent of the state of matter during the time of observation. The bottom arrangement shows how the extinction of light by liquid fuel is captured using Diffused Back-Illumination (DBI) imaging as proposed in [3].
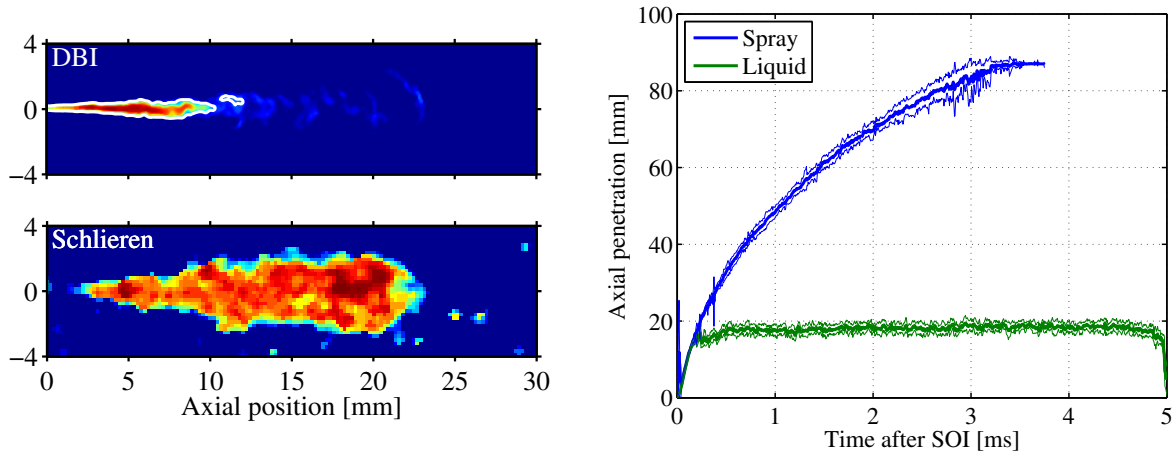

Figure 2: Left top: individual DBI image at 0.3 ms after Start Of Injection (SOI) with a contour at a fixed extinction value to determine a time-resolved liquid penetration. Left bottom: Schlieren image at the same time-instance as the DBI recording during a different experiment. Right: time-resolved penetration of spray and liquid. More details are provided in the text.

Results and future work

The left images of Figure 2 shows post-processed snapshots of individual experiments performed with DBI and Schlieren, as indicated in upper left corners. The right image shows time-resolved results of multiple experiments with the standard deviation indicated by a decreased line thickness. For the DBI experiments, a fixed extinction value is used to determine the liquid penetration which is indicated with a white contour in the example image. To validate these values, a time-averaged image is computed as well, in which a line is fitted through the decreasing extinction over the axial position. This gives a better estimation of the quasi-steady liquid-length value at the intersection of this line with a point on the axis of zero extinction. For the Schlieren experiments, a different approach is used since there is a constant propagation of the spray and an interfering background resulting from the density gradients at the vessel windows. Therefore, at every point in time, the previous frame is subtracted from the image under investigation to determine the spray penetration accurately. The right plot of Figure 2 illustrates how good reproducibility is achieved between individual experiments with an expected overlap in axial penetration before the spray starts to evaporate. These preliminary results provide an important initial step towards the study of spray wall-interaction in both experiments and numerical simulations. The next step is to extend the created database with reacting experiments to characterize the flame structures and associated parameters. Subsequently, a wall-insert will be placed inside the vessel to study the interaction between the (reacting) fuel-spray and such an obstruction. In the meantime, numerical simulations are carried out with the available data to support the work.

References

[1] Baert, R., Frijters, P., Somers, B., Luijten, C. et al., "Design and Operation of a High Pressure, High Temperature Cell for HD Diesel Spray Diagnostics: Guidelines and Results," SAE Technical Paper 2009-01-0649, 2009, doi:10.4271/2009-01-0649.

[2] "Engine Combustion Network internet library." http://www.sandia.gov/ecn/

[3] Manin, J., Bardi, M. and Pickett L.M., "Evaluation of the Liquid Length via Diffused Back-Illumination Imaging in Vaporizing Diesel Sprays,", *COMODIA*, 2012.

Modelling Tar Conversion in a Partial Oxidation Reactor Using Flamelet Generated Manifolds

J.C.A.M. Pennings[1,*], J.A. van Oijen[1], T. Kuipers[2], F. Melkert[2]

[1]*Eindhoven University of Technology, Department of Mechanical Engineering*
[2]*De Jong Combustion B.V.*

Motivation

The amount of fossil fuels on planet earth is diminishing, while its consumption increases rapidly [1]. To ensure our energy supply, a gradual transition to other energy sources is needed. Renewable energy may play a significant role in this transition, with its additional advantage of being carbon dioxide neutral. Several technologies have been developed, including windmills and solar cells. However, the problem with these technologies is the storage of the produced electricity. The solution for this problem may lie in the transformation of electricity into chemistry: Power-to-Gas [2]. In Delfzijl (Groningen, NL.) the first large scale, completely integrated Power-to-Gas installation will be build, in which green power is converted into hydrogen and pure oxygen via electrolysis. As schematically shown in figure 1, the produced hydrogen can be used as a raw material for the chemical industry. The pure oxygen can be used to gasify torrefied biomass into syngas; a valuable source for the chemical industry mainly consisting of carbon monoxide and hydrogen.
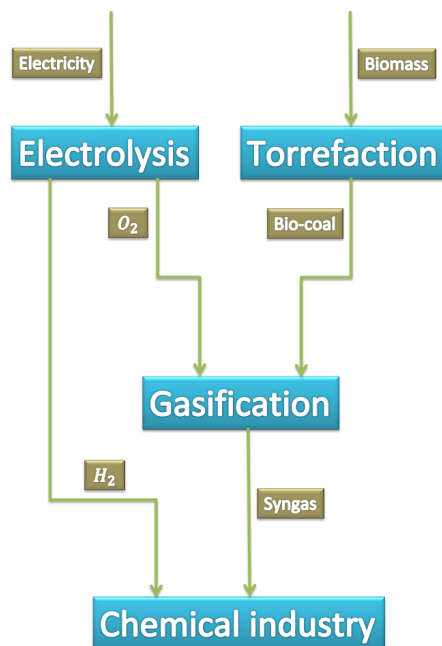

Figure 1: Schematic representation of the Power-to-Gas principle.

*Corresponding author: j.c.a.m.pennings@student.tue.nl

The gasification from biomass into syngas occurs in two stages: first torrefied biomass is converted under influence of heat into gas in a pyrolysis unit, and afterwards the arisen gasses are partially oxidized in a partial oxidation reactor, which will be developed by the A. de Jong Group. These gasification processes have been extensively investigated [3][4], and the major problem is the formation of tars in the pyrolysis unit. Tar is very easy to condense and difficult to remove, causing fouling in downstream processes. Several methods have been developed to reduce the tar content in syngas, including thermal conversion, catalytic cracking, mechanical separation and partial oxidation. It has been proven that partial oxidation can reduce the tar content significantly [5]. In this process, tars and other volatiles are partly oxidized, while the released heat is used for thermal cracking of the remaining pollutants. In this way, tar content can be reduced and converted into non-condensable gasses.

However, the elementary processes occurring at partial oxidation are not yet fully understood, and research is needed to ensure a satisfying tar conversion rate. Therefore, a 500 kW pilot plant has been built in order to verify the working principle of biomass gasification in a two-stage gasifier. However, satisfactory experimental results on a pilot plant is no guarantee for equal results on a full-scale installation. Therefore, experimental data from this pilot plant can be used to validate the modelling of tar conversion. When validated, numerical models can be used to predict tar conversion on a full-scale installation. Hence, the purpose of this study is to validate a numerical model on tar conversion in the pilot version of the partial oxidation reactor in order to predict tar conversion on a full-scale installation.

Method

Experiments on the pilot plant will be conducted according to the Design Of Experiments (DOE) principle, where measurement points are selected carefully by varying relevant factors simultaneously. These factors should be controllable, and chosen prior to the experiments. In tar conversion, temperature and residence time are of great importance [5]. In the two-stage gasifier, there are two important temperatures: the pyrolysis and partial oxidation temperature; the temperature of the pyrolysis reactor determines the amount

and composition of tars that have to be destructed under influence of the partial oxidation temperature. Both temperatures are measured, and can be controlled by varying the mass flow of oxygen into the reactors. Thus, these temperatures can be chosen as factors. The residence time determines the period for the tars to be subjected to these temperatures, and can be controlled via the mass flow of biomass through the system. Since the actual residence time is not measured, the mass flow of biomass is chosen as a factor.

As can be seen in figure 2, the measurement points are distributed in a cubic design space. On the axes the factors can be found, and in the middle of the cube there are three center measurement points to verify the reproducibility of the experiment. This approach enables the ability to map tar conversion as a function of the three chosen factors. A statistical model can be derived, and this model can be compared to numerical modelling results.
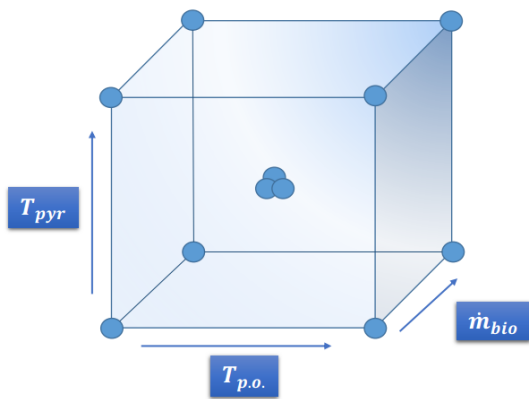

Figure 2: Full factorial DOE design.

To obtain numerical tar conversion data, a three-dimensional model will be constructed in ANSYS Fluent. Since tar includes many species with different behaviour, an extensive reaction mechanism is needed to describe their formation and destruction. The reaction mechanism of Ranzi, consisting of 185 species and 6445 reactions, has been proven to predict tar conversion quite well [6]. So, this mechanism is chosen to describe the elementary processes. Since it is too extensive for direct integration, the Flamelet Generated Manifolds (FGM) reduction technique is used. In this approach, prior to the combustion simulation, a database of thermochemical variables (manifold) is generated as a function of control variables for given initial conditions. During run-time of ANSYS Fluent the transport equations for these control variables are solved, together with the momentum equations. All relevant combustion data can be retrieved from the pre-determined manifold, which reduces computation time significantly [7]. By simulating the same measurement points in a numerical model, a similar statistical model can be derived. Then, trends from the experimental and numerical modelling results can be compared, and conclusion can be drawn on the ability to model tar conversion in a partial oxidation reactor.

Results

Since experimental data is not yet available, results will not be presented.

References

[1] Mohr, S.H., Wang, J., Ellem, G., Ward, J., Giurco, D. (2014). *Projection of world fossil fuels by country*. Sydney University of Technology.

[2] Power-to-Gas. In *A. Hak*. *Consulted on* 21 February 2015 at 8:21. `http://www.a-hakpark.nl/power-to-gas`

[3] Kiel, J.H.A. (2004). *Primary measures to reduce tar formation in fluidised-bed biomass gasifiers*. Energieonderzoek Centrum Nederland.

[4] Milne, T.A., Evans, R.J. (1998). *Biomass Gasifier "Tars": Their Nature, Formation, and Conversion*. National Renewable Energy Laboratory.

[5] Chhiti, Y., Peyrot, M., Salvador, S. (2013). *Soot formation and oxidation during bio-oil gasification: experiments and modeling*. Ecole des Mines d'Albi-Carmaux.

[6] Faravelli, T., Goldaniga, A., Ranzi, E. (1998). *The Kinetic Modeling of Soot Precursors in Ethylene Flames*. Politecnico di Milano.

[7] Donini, A. (2014). *Advanced Turbulent Combustion Modeling for Gas Turbine Application*. Eindhoven University of Technology.

Reintjes M.*, Ramaekers W.J.S., van Oijen J.A., Tap F.A.
'Combustion in Swirling Flows, Modelling of Premixed Turbulent Combustion in Swirling Flows using Large Eddy Simulations and Tabulated Chemistry'
Technische Universiteit Eindhoven, (2015)

Abstract

Modern industrial burners often operate under lean (sub-stoichiometric) conditions. This reduces the production of harmful pollutants, but decreases the stability of combustion. Flame stabilization is achieved by introducing a swirling motion to the flow. This motion creates a recirculation zone that transports heat and active chemical species back to the flame front. However, predicting the stability and behaviour of these flames is not straight-forward. The swirling flow-flame interaction is very complex and the flow is often highly turbulent. Modelling this phenomenon can be achieved by running a Large Eddy Simulation (LES), an unsteady numerical technique in which the large turbulent flow structures are resolved and smaller ones are modelled.

In this work, the problem of modelling a turbulent swirling reacting flow is tackled by first separating the problem into two test cases; one for the turbulent swirling flow and the other of the combustion chemistry. In the first case, a cold turbulent swirling flow has been modelled with time-dependent LES using the open source CFD package OpenFOAM®. Based on comparisons to experimental data, the LES results accurately predicted velocity profiles as well as key flow features, such as the recirculation zone and the Precessing Vortex Core (PVC).

For the second case a Direct Numerical Simulation (DNS) of a laminar premixed lean methane/air flame has been computed using the Flamelet-Generated Manifold (FGM) technique [1]. This technique solves the chemistry solution offline and stores it in a table to be used during the simulation. The implementation into the CFD has been achieved using Tabkin© by Dacolt [2]. The effectiveness of FGM is demonstrated by comparing the results of the laminar flame to detailed chemistry solutions. The results are nearly identical, with the FGM result being computed almost 7 times faster. Such a speedup is crucial when attempting to model larger practical flames.

Finally, a numerical study is conducted on the Cambridge-Sandia Swirl Burner [3] using the 'best-practice' methods from the two cases above. The results of this simulation campaign have been presented on the poster. Without tuning model parameters and within reasonable computational effort, the model is able to correctly predict both the swirling flow and important flame characteristics, such as the flame angle. Also, as a large part of the turbulence is resolved by the LES approach, both average values as well as fluctuations in velocity, temperature and equivalence ratio are accurately predicted. The results of this simulation campaign showcases the potential of the model for further developments in gas turbine combustors.

[1]   Van Oijen J. A., *"Flamelet-Generated Manifolds: Development and Application to Premixed Laminar Flames"*, Technische Universiteit Eindhoven, (2002)

[2]   Tap F., Schapotschnikow P., *"Efficient Combustion Modeling Based on Tabkin CFD Look-up Tables: A Case Study of a Lifted Diesel Spray Flame"*, SAE 10.4271/2012-01-0152 (2012)

[3]   M.S. Sweeney, S. Hochgreb, M.J. Dunn, R.S. Barlow, *"The structure of turbulent stratified and premixed methane/air flames II: Swirling flows"*, Combustion and Flame. 159 2912–2929, (2012)

Fate of Forgotten Fuel:
High-speed Laser-Induced Incandescence

Robbert Willems, r.c.willems@student.tue.nl
Peter-Christian Bakker, p.c.bakker@tue.nl
Nico Dam, n.j.dam@tue.nl

Eindhoven University of Technology

Conventional diesel combustion in compression ignition (CI) engines has become an established combustion technique by more than a century of dedicated research. Although such engines have superior efficiency over gasoline engines, they are plagued by harmful emissions of soot particles and nitrogen oxides (NO_x). Soot emissions have dropped more than an order of magnitude in the last decade, mainly due to improved fuel injection equipment and complex after-treatment systems. However, formation and oxidation processes, as well as radiative heat losses and their impact on engine efficiency, are still not well understood.

This work aims to qualitatively measure the in-cylinder soot processes on an optically-accessible CI engine using the well-established Laser-Induced Incandescence (LII) technique, albeit at high-repetition rate. The intention is to study the relatively unknown late-burn phase, i.e. after the injection has ended. Phase-averaged data does not provide all information here, because of the turbulent nature of the diesel combustion process. Measurement repetition rates in the order of several kilohertz enable the acquisition of crank-angle resolved data within a single combustion cycle. Ultimately, finding ways to speed up this late-phase combustion might be the key to improve engine efficiency and to reduce the emission of soot.

Applying a multi-kHz system gives rise to several challenges, such as step-wise sublimation or changes in morphology, since soot particles possibly experience multiple laser pulses. Additionally, retrieving information on soot volume fraction tends to be more difficult in engines because of changing ambient temperatures and increased conduction rates. Solutions for reducing the above mentioned effects are often contradicting, which further complicates experimental procedures.

Measurements on an atmospheric co-flow burner were done prior to engine experiments in order to identify possible problems with step-wise sublimation and other multiple exposure effects. It was found that, in this type of flame, a fluence around 0.1 J/cm^2 gives the best balance between the signal-to-background ratio, soot sublimation and local gas heating. This fluence, however, is well below the plateau regime of LII which creates additional problems with the interpretation of the signal when large temperature and density gradients, as well as a high degree of turbulence are present.

The many pitfalls with (high-speed) LII and the strategy to tackle these problems are discussed, and eventually some qualitative results are shown. The technique is considered feasible for qualitative measurements, but the balance between fluence, signal detection and changes to soot particle size and morphology was shown to be extremely delicate.